



NTNU – Trondheim
Norwegian University of
Science and Technology

Structure - Slug Flow Coupling: Small Scale Experiments with Submerged Flexible Pipes

Amr Khalil Hemed Khalil
Mohamed Hemed

Natural Gas Technology

Submission date: June 2015

Supervisor: Ole Jørgen Nydal, EPT

Norwegian University of Science and Technology
Department of Energy and Process Engineering



NTNU – Trondheim
Norwegian University of
Science and Technology

Structure - Slug Flow Coupling: Small Scale Experiments with Submerged Flexible Pipes

Mohamed Hemed, Amr

Trondheim, June 2015

Master of Natural Gas Technology

Supervisor: Ole Jørgen Nydal

Research Advisors: Nicolas La Forgia & Joaquin Vieiro

Norwegian University of Science & Technology

Faculty of Engineering Science and Technology (IVT)

Department of Energy and Process Engineering

EPT-M-2015-58

MASTER THESIS

for

Student Amr Mohamed Hemeda

Spring 2015

Structure - slug flow coupling: small scale experiments with submerged flexible pipes*Struktur – slug strøm kobling; små-skala forsøk med fleksible rør***Background and objective**

An ongoing research project concerns the coupling between the internal two phase flow and the structural dynamics of flexible pipes. The project is computational, where a 1D structural model for the pipe is integrated into a dynamic flow model. The structural model is formulated in 3D space, and the flow model is based on a slug tracking method, giving non-diffusive propagation of gas-liquid fronts.

An experimental project is proposed in support of the modelling work. Some small scale experiments were investigated in a project work, where severe slugging was established in a setup with a flexible pipe mounted with springs, allowing for some pipe movement during the severe slugging cycles. The movement was quantified from markers attached to the pipe and digital image analysis from a video recording.

The small scale experiments were useful, and experiments with a pipe submerged into water would be the next step. A case with a two way coupling between the internal flow and the pipe dynamics is suggested. This can be a floating pipe, attached with a spring at the pipe outlet. At severe slugging conditions, the pipe structure would then be unstable; liquid accumulation in a bend would lead to the bend sinking and give further liquid accumulation, until blowout occurs and the pipe risers again. The same image analysis method can be applied for the submerged pipe, provided visual access through transparent walls.

The experiments will provide data for comparisons with the numerical simulations.

The following tasks are to be considered:

- 1 Design and construction of a water channel for experiments with flow in submerged pipes.
- 2 Establishment of a test setup: instrumentation, pump, pipes, separator etc
- 3 Experiments at severe slugging conditions
- 4 Comparisons with simulations.
- 5 Reporting and suggestions for further work.

-- ” --

Within 14 days of receiving the written text on the master thesis, the candidate shall submit a research plan for his project to the department.

When the thesis is evaluated, emphasis is put on processing of the results, and that they are presented in tabular and/or graphic form in a clear manner, and that they are analyzed carefully.

The thesis should be formulated as a research report with summary both in English and Norwegian, conclusion, literature references, table of contents etc. During the preparation of the text, the candidate should make an effort to produce a well-structured and easily readable report. In order to ease the evaluation of the thesis, it is important that the cross-references are correct. In the making of the report, strong emphasis should be placed on both a thorough discussion of the results and an orderly presentation.

The candidate is requested to initiate and keep close contact with his/her academic supervisor(s) throughout the working period. The candidate must follow the rules and regulations of NTNU as well as passive directions given by the Department of Energy and Process Engineering.

Risk assessment of the candidate's work shall be carried out according to the department's procedures. The risk assessment must be documented and included as part of the final report. Events related to the candidate's work adversely affecting the health, safety or security, must be documented and included as part of the final report. If the documentation on risk assessment represents a large number of pages, the full version is to be submitted electronically to the supervisor and an excerpt is included in the report.

Pursuant to "Regulations concerning the supplementary provisions to the technology study program/Master of Science" at NTNU §20, the Department reserves the permission to utilize all the results and data for teaching and research purposes as well as in future publications.

The final report is to be submitted digitally in DAIM. An executive summary of the thesis including title, student's name, supervisor's name, year, department name, and NTNU's logo and name, shall be submitted to the department as a separate pdf file. Based on an agreement with the supervisor, the final report and other material and documents may be given to the supervisor in digital format.

- Work to be done in lab (Water power lab, Fluids engineering lab, Thermal engineering lab)
 Field work

Department of Energy and Process Engineering, 14. January 2014



Olav Bolland
Department Head



Ole Jorgen Nydal
Academic Supervisor

Research Advisor: Nicolas La Forgia, Joaquin Vieiro

Abstract

Multiphase flows include several flow regimes that exist with different conditions. The time varying forces in flexible pipes conveying two-phase flows results in very dynamic structural behavior. These varying forces contribute to fatigue stresses which have a major effect on a riser life time.

Studying the dynamic response of flexible pipes conveying two-phase flows can reveal crucial information regarding induced vibrations and oscillations in risers. These information can be utilized in understanding operational hazards with flexible risers in oil and gas industry.

An experimental investigation of flexible pipes is carried out in the lab. A small scale experimental loop was designed for testing structural behavior of flexible pipes conveying air and water two-phase flow. Experiments were recorded and video processing techniques were utilized for analyzing structural response.

The amplitudes of structural oscillations were measured for several cases at different pipe lengths and flow superficial velocities. Two main geometries were investigated, a cantilever pipe in vertical and horizontal direction and a geometry representing a riser collapse inspired by a real accident from oil and gas industry.

The experimental results were compared to numerical simulations from a structural dynamic analysis code. The work produced in this thesis was presented for publishing as a part of scientific paper shown in Appendix (A).

Acknowledgement

Project / research funded by VISTA – a basic research program and collaborative partnership between The Norwegian Academy of Science and Letters and Statoil.

I would like to express my sincerest thanks and appreciation to my supervisor Professor Ole Jørgen for his encouragement, support and valuable guidance through the year.

I owe my deepest gratitude to Joaquin Vieiro for his endless support and assistance. His guidance into the analysis of results has been essential during this work.

Finally, I am deeply grateful to Nicolas La Forgia for his guidance and help in the lab, making it possible to carry out the experiments efficiently.

Contents

Abstract	i
Acknowledgement.....	ii
List of Figures	v
Chapter (1): Introduction.....	1
1. Background.....	1
2. Scope.....	2
3. Scientific Contribution.....	2
4. Motivation.....	2
Chapter (2): Theoretical Background.....	4
1. Multiphase Flow Regimes	4
2. Severe Slugging in Risers	5
3. Literature Review.....	6
3.2 – Cantilever flexible pipe	6
3.2 – DWH riser	8
Chapter (3): Measurements & Experimental Work	9
1. Description.....	9
2. Experimental Apparatus.....	9
2.1 – Cantilever experimental geometries.....	11
2.2 - DWH riser experimental geometry	12
3. Video Processing	13
4. Bending Stiffness	14
5. Flow Rates Measurements	16
Chapter (4): Cantilever Hose Experiments	18
1. Horizontal Geometry	18
2. Vertical Geometry.....	23

3. Discussion	24
Chapter (5): DWH Riser	26
1. DWH Riser Case Description	26
1.1 – Double and single peak pattern	27
2. Experimental and simulation results	28
2.1 – Case (1).....	28
2.2 – Case (2)	32
2.3 – Case (3)	33
2.4 – Case (4)	34
3 Discussion	35
Conclusion.....	36
Recommended Future Work	37
References	38
Appendix (A): Presented Paper for Publishing	40

List of Figures

Figure (1. 1): DWH riser lying on seabed after drilling rig sinking [4].....	3
Figure (2. 1): Multiphase flow regimes in vertical and horizontal pipes	4
Figure (2. 2): Severe slugging cycle in risers - [6].....	6
Figure (3. 1): Mini-loop instrumentation box	9
Figure (3. 2): Compressor connected to high pressure tank.....	10
Figure (3. 3): a) Needle water adjustment valve b) Water pump	10
Figure (3. 4): 1- Water supply tank, 2- Centrifugal pump, 3- High pressure Tank, 4- Compressor, 5- Ball valve, 6- Digital air flow meter, 7- Low pressure buffer tank, 8- Needle valve, 9- Analog liquid flow meter, 10- Air & water mixer	11
Figure (3. 5): Vertical and horizontal geometries of the cantilever hose experiments	12
Figure (3. 6): DWH riser geometry implemented in the lab	12
Figure (3. 7): Tank used for DWH riser experiments	13
Figure (3. 8): Under-construction tank for future experiments with floating pipes, dimensions: 4 x 0.5 x 1.4 meters	13
Figure (3. 9): Points detected by the MATLAB code	14
Figure (3. 10): Real scale image for experiments	14
Figure (3. 11): Pendulum experiment for estimating bending stiffness.....	15
Figure (3. 12): Pendulum oscillations for hoses (1) and (2).....	15
Figure (3. 13): Experimental and simulation results for estimating bending stiffness – [10]..	16
Figure (4. 1): Red detected point's distances from fixed terminal.....	18
Figure (4. 2): Trajectory of point's oscillation displacement in both vertical and horizontal directions for case (1).....	19
Figure (4. 3): Number of strokes travelled by point (5) for case (1) with reference to upper left corner of every frame of the video	19
Figure (4. 4): The relation between vertical and horizontal displacements of points (1) to (5) relative to distance of each detected point from fixed one.....	20
Figure (4. 5): Ellipse motion pattern made by points (1), (2) and (3).....	20
Figure (4. 6): Perturbations of the free end for case (1), red arrow indicates distance displaced by the hose due to liquid slug flow out	21
Figure (4. 7): Perturbations of hose free end for cases (2) and (3); the curve is smoother indicating shorter step displacement for the perturbations.....	21
Figure (4. 8): Strokes travelled by point (5) for cases (1), (2) and (3).....	22

Figure (4. 9): Trajectory of half stroke travelled by points in case (4)	22
Figure (4. 10): Vibrations of points (3), (4) and (5) for case (5) with 50 cm length of hose ...	23
Figure (4. 11): Hose free end detected point	24
Figure (4. 12): Vibrations amplitude for cases (1), (2) and (3) of vertical geometry.....	24
Figure (4. 13): Trajectory of experimental and simulation results for case (1).....	25
Figure (5. 1): Main oil slug accumulating in upstream section of buoyant loop [4].....	26
Figure (5. 2): Oil flowing towards top pushing the buoyant loop to sink towards seabed [4].	26
Figure (5. 3): Buoyant loop resting on seabed and stratified flow pattern emerges [4].....	27
Figure (5. 4): Buoyant loop rising again after filling with gas [4]	27
Figure (5. 5): Double peak behavior for flow output [4]	27
Figure (5. 6): Stratified flow splitting into two oil slugs – double peak behavior	28
Figure (5. 7): Liquid filling buoyant loop for case (1)	29
Figure (5. 8): Elongated bubbly flow prior to liquid accumulation	29
Figure (5. 9): Stratified flow starting after liquid accumulation	30
Figure (5. 10): Slugging behavior for case (1)	30
Figure (5. 11): Liquid slug filling up the buoyant part and pushing it down towards tank bottom.....	31
Figure (5. 12): Simulation results for case (1).....	31
Figure (5. 13): Slugging behavior for case (2) showing flat troughs with small pointed part .	32
Figure (5. 14): Left image shows slug filling until point (2), right image shows slug passed point (2) pushing the buoyant loop to a lower depth.....	32
Figure (5. 15): Simulation results for case (2).....	33
Figure (5. 16): More chaotic motion pattern of case (3)	33
Figure (5. 17): Simulation results for case (3) showing similar chaotic behavior and less displacement amplitudes	34
Figure (5. 18): Motion pattern of case (4) with more uniform behavior as in cases (1) and (2)	34
Figure (5. 19): Simulation results for case (4).....	35

Chapter (1): Introduction

An offshore field development involves many components and facilities for processing and transport of oil & gas. Risers are a main component of any offshore field responsible for transferring well fluids from seabed to surface facility. Risers can be classified into two main types; rigid risers and flexible risers. Flexible risers are multi-layered composite flexible structures used to connect subsea equipment to floating production units.

Since 1986, flexible risers have gained more concern in Norwegian petroleum production. With the increase in number of floaters used in Norwegian Continental Shelf (NCS), the number of flexible risers utilized increased to 326 risers by 2013. [1]

There is always a large demand for studies on dynamic behavior of flexible risers relative to internal and external forces. The internal flow forces caused by two-phase flow regimes may result in vibrations or oscillation in risers. The presented work here provides an experimental investigation of dynamic behavior of flexible risers relative to internal two-phase flow. The results can be used for verifying software simulations in the future.

1. Background

The reliability and safe operation of a riser system requires a broad assessment of all risks and hazards associated with its operation. Vibrations in flexible risers may lead to reduction in field production and even shutdown in some cases and therefore large financial losses.

Marulk field has experienced a temporary shutdown in October, 2012 due to vibration in Norne FPSO gas export riser [2]. Such shutdowns or reduction in production result in massive financial losses.

It is important to understand the interaction between dynamic behavior of risers and internal flows. This may provide tools for eliminating failures and hazards associated with risers operation and allow for investigating breakdowns and operational accidents.

On April 20, 2010, the world was shocked by the explosion of Deepwater Horizon (DWH) drilling rig operated by BP near the coast of Louisiana, US. The collapse of flexible riser connected to DWH rig resulted in the largest oil spill in US history. The initial estimation of flow rate on the day the oil was capped was 53,000 BOPD.

An Oscillating motion in a buoyant part of the riser implemented that slug flow have existed in the riser. The presence of slug flow in the riser had a significant effect in reducing the financial penalties paid by BP [3].

2. Scope

The thesis aims to investigate the dynamic behavior of flexible pipes relative to different gas and liquid superficial velocities. A mini-loop experimental apparatus is to be designed for carrying out small scale experiments in the lab with two-phase air and water supply. The dynamic behavior of pipes is to be recorded and analyzed. Experimental data are investigated in comparison with software simulations.

The work was planned to include experimental investigation of three major geometries. The geometries include cantilever hose, floating pipe connected to external force and a riser oscillating in a tank representing the DWH riser incident.

For investigating the floating pipe experiment, a large tank needed to be fabricated. As the tank was not fabricated on time, the experiment was postponed to future work.

3. Scientific Contribution

The experimental data produced was published as a part of scientific paper presented at 8th National Conference on Computational Mechanics – MekIT'15. The data from experiments was compared to numerical simulations from structural dynamic analysis code. The simulations data from the code was provided by Joaquin Vieiro as part of his PhD work. The coupled work resulted in the produced paper draft in Appendix (A). [10]

4. Motivation

Fluid-elastic instabilities are large amplitude oscillations of pipes due to increase of flow velocity beyond certain value known as critical velocity [13]. Many researchers investigated the fluid-elastic instability of cantilever flexible pipes conveying single phase flow.

However, there are not enough studies considering the two phase flow in which many pipes are subjected to. It was necessary to conduct experiments for revealing the effect to two phase flows in cantilever pipes.

In April – 2010, an explosion of the Deepwater Horizon (DWH) drilling rig led to riser disconnecting from the rig. The collapsed riser extended on the seabed lying over the sinking rig and forming the geometry shown in figure (1.1).

Remotely operated vehicles (ROV) videos have shown an alternating dark and light colored fluid discharged from the riser end. Investigation of the videos concluded that the alternating fluid discharge was slug flow where dark colored fluid was oil dominated flow and light colored was gas dominated flow. An oscillating motion of the buoyant loop portion of the riser was linked to the existence of slug flow [4].

Small scale experiments were conducted for the aim of comparing the physics behind structural behavior of the riser in real scale and small scale experimental apparatus in the lab. The experimental data was compared to numerical simulations and presented in an internal report at the energy and process department, NTNU. The results from experiments and simulations are planned to be published in future.

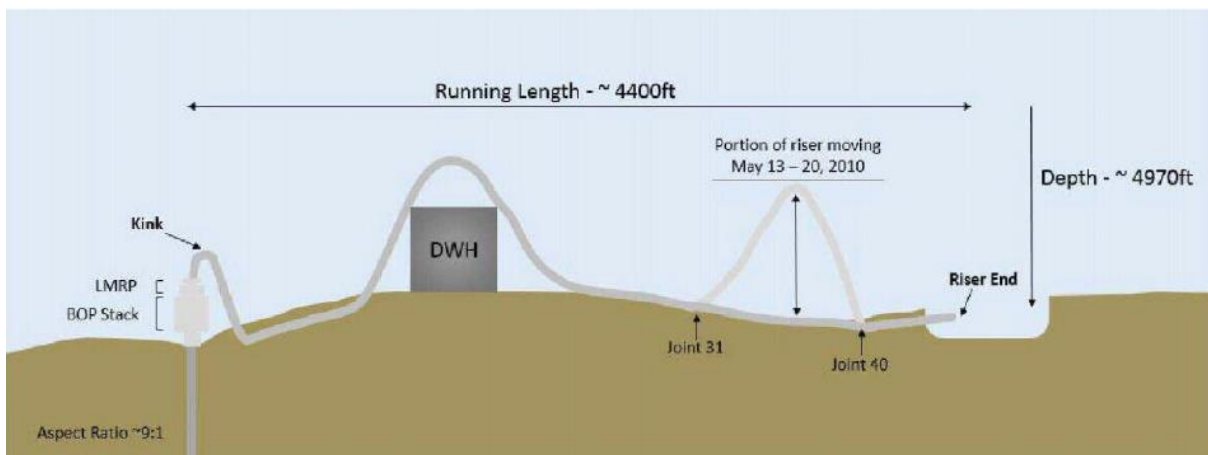


Figure (1. 2): DWH riser lying on seabed after drilling rig sinking [4]

Chapter (2): Theoretical Background

1. Multiphase Flow Regimes

Flow regimes have the major effect on internal forces inducing structural dynamic behavior. Depending on pipe orientation (vertical, horizontal and near horizontal), fluid properties and flow rates, several flow regimes can emerge in a system. The major flow regimes relative to thesis work are described below.

Stratified Flow: a flow pattern recognized by liquid flowing at the bottom of the pipe and gas flowing on top. At low flow rates, the shape of interface between the two phased takes a smooth shape. However, increasing the gas flow rates results in the appearance of waves [5].

Annular Flow: annular flow can emerge as a gradual change from stratified flow. Drops created by atomization of irregular waves can deposit on the pipe wall creating a turbulent film. It is recognized by a gas core in the middle with liquid film at the walls [5].

Bubble Flow: bubble flow can appear in the form of dispersed bubbles at high liquid flow rates in horizontal pipes or bubbly flow at low flow rates in vertical pipes [5].

Slug Flow: slug flow can be defined as an alternating sequence of bubbles and liquid slugs. From an operational perspective, slug flow can be classified into two types; small scale slugging such as hydrodynamic slug flow and large scale slugging such as severe slugging [5].

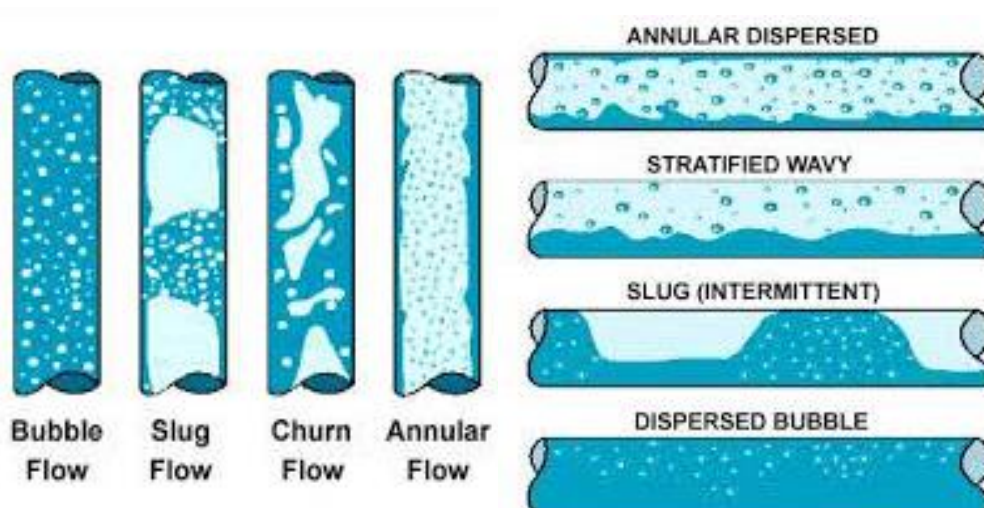


Figure (2. 1): Multiphase flow regimes in vertical and horizontal pipes

2. Severe Slugging in Risers

Severe slugging is a very dynamic phenomenon recognized by the formation and cyclic production of long liquid slugs followed by gas blowdown. [6]

Severe slugging causes rapid changes in mass distribution and pressure fluctuations along risers. This leads to vibrations which results in time varying stresses. These stresses may cause damages to risers due to fatigue, excessive bending or local buckling [7].

There are certain conditions that induce the occurrence of severe slugging. The geometry has to include a low point such as a bend for liquid accumulation. With sufficient gas compressibility upstream the low point and suitable gas and liquid flow rates, the severe slugging cycle occurs.

Figure (2.2) demonstrates the penetration of gas and liquid through different flow stages of a severe slugging cycle. A severe slugging cycle includes the following stages;

Slug formation; liquid accumulates at the bottom of the riser and blocks the gas passage; pressure increases and compresses the gas in the pipe.

Slug production; as liquid level reaches the top of the riser, the pressure reaches its maximum value and only liquid flows into the riser.

Blowout; as the gas continues to flow in, the liquid accumulation is pushed to the bottom of the riser and there by initiating the blowout stage.

Blow down; the gas penetrating into the riser column makes it lighter and decreases its pressure. Gas reaches the top of the riser until its passage is free causing violent expulsion and rapid decompression that brings the process to slug formation again [6].

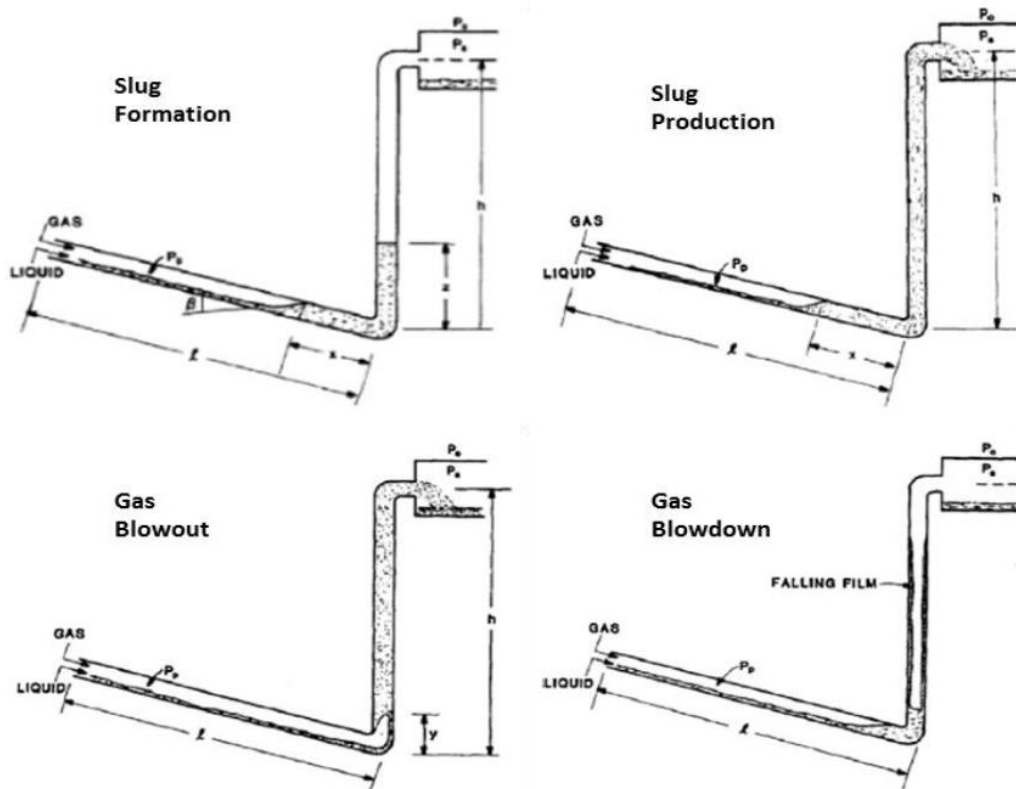


Figure (2. 2): Severe slugging cycle in risers - [6]

3. Literature Review

In 2012, Ortega et al. [8] used two softwares for simulating the response of risers due to internal flow. A high level architecture (HLA) federation was created for allowing the interaction between the two softwares. A HLA federation is an object oriented common technical architecture aims at providing interoperability between different federates such as simulations [9].

The first software is SLUGGIT, a two phase flow code written in C++ which was used to simulate dynamic slug flow. Results from SLUGGIT were coupled with RISANANL which is a FORTRAN program for static and dynamic structural analysis of slender marine structures. The work resulted in a code that was able to predict the response of a lazy wave riser based on internal slug flow. The study investigated the movements of some nodes in the riser geometry [8].

3.2 – Cantilever flexible pipe

(T. B. Benjamin, 1960) introduced a general theory covering the free motions of a cantilever chain of articulated rigid pipes conveying incompressible, constant and single phase flow. He established Lagrangian equations where dependent variables are potential and kinetic energies

of the pipes and space enclosed by them. A continuously flexible elastic tube was considered an extreme case of the presented theory as number of degrees of freedom is infinite. [16]

(M. P. Paidoussis, 1970) introduced a two parts study on the dynamics of cantilever tubes conveying single phase flow. In Part I, he developed an equation for small lateral motions formulating the fluid-elastic instability for internal flows in cantilever tubes.

$$EI \frac{\partial^4 y}{\partial x^4} + (M + m)g \left((x - L) \frac{\partial^2 y}{\partial x^2} + \frac{\partial y}{\partial x} \right) + MU^2 \frac{\partial^2 y}{\partial x^2} + 2MU \frac{\partial^2 y}{\partial t \partial x} + (M + m) \frac{\partial^2 y}{\partial t^2} + EI \frac{\mu}{\Omega} \frac{\delta}{\delta t} \left(\frac{\partial^4 y}{\partial x^4} \right) + k \frac{\partial^2 y}{\partial t^2} = 0 \quad (2.1)$$

Where;

***EI:** tube flexural rigidity, **y:** lateral deflection of the tube, **x:** longitudinal coordinate, **M:** mass of fluid per unit length, **m:** mass of tube per unit length, **g:** gravitational acceleration, **L:** length of the tube, **U:** average flow velocity, **μ :** structural damping coefficient, **Ω :** circular frequency, **t:** time and **k:** dimensionless viscous damping coefficient*

The equation demonstrates involved forces; flexural force, pressure & tension, centrifugal force, Coriolis force, inertia force, structural damping force and viscous damping force. The equation is developed considering single phase flow.

Part II included experiments for demonstrating the dynamic behavior of vertical cantilever tube conveying single phase flow. The tubes were tested in two configurations; hanging down and standing upright. [15]

(C. Monette & M. J. Pettigrew, 2004) conducted a series of experiments for studying fluid-elastic behavior of flexible pipes when subjected to two-phase flow. The experiments involved several pipes with different diameters, lengths and flexural rigidities. The results were compared to theoretical formulation.

The formulation was developed based on equation (2.1) introduced above. In the case of two phase flow as in the experiments, the difference between gas and liquid velocities is significant. Therefore, the Coriolis and centrifugal forces of each phase will be considered separately. Accordingly, equation (2.1) would be modified to the form;

$$EI \frac{\partial^4 y}{\partial x^4} + (\sum_k M_k + m)g \left((x - L) \frac{\partial^2 y}{\partial x^2} + \frac{\partial y}{\partial x} \right) + \sum_k M_k U_k^2 \frac{\partial^2 y}{\partial x^2} + 2 \sum_k M_k U_k \frac{\partial^2 y}{\partial t \partial x} + (\sum_k M_k + m) \frac{\partial^2 y}{\partial t^2} + EI \frac{\mu}{\Omega} \frac{\delta}{\delta t} \left(\frac{\partial^4 y}{\partial x^4} \right) + k \frac{\partial^2 y}{\partial t^2} = 0 \quad (2.2)$$

Where M_k and U_k represent the mass and velocity of each phase respectively. The work concluded that stronger turbulence in two-phase flow resulted in larger vibrations compared to single phase. [12]

(J. Yoon et al., 2006) studied the free vibration and flow-induced flutter instability of cantilever carbon nanotubes influenced by internal moving fluid. They defined flutter instability as a phenomenon of growing amplitude of vibration with time after critical flow velocity is achieved. The study assumed a uniform steady state, single phase and incompressible flow with uniform flow velocity. Their results showed that critical flow velocity inducing flutter instability may exist within practical significance. [17]

(R. W. Gregory & M. P. Paidoussis, 1966) introduced a theoretical model including a parameter ' β ' defined as the ratio mass/length of fluid conveyed in a pipe to mass/length of pipe material. Oscillations were defined by dimensionless circular frequency parameter ' ω ' relating oscillations to flexural rigidity. They solved equations of motions and compared them to experimental results of single phase flow. [14]

(R. A. Ibrahim, 2011) reviewed some of the researches conducted on single and two-phase flows in pipes. Some researchers investigated the effect of two-phase cross flow on tube bundles but not much was done on axial two-phase flow in a single tube. [20]

3.2 – DWH riser

A report investigating the incident was provided by Dr. Michael Zaldivar [4]. His report confirmed that the oscillating behavior of buoyant part of the riser is related to slug flow. Using LedaFlow as multiphase flow simulator, Zaldivar was able to estimate the flow rates of oil leakage. He relied on programming interface for changing the buoyant loop elevation during LedaFlow simulations and calculates corresponding flow rates. [4]

Chapter (3): Measurements & Experimental Work

1. Description

The cantilever hose and DWH cases were investigated on small scale geometries in the lab. A mini-loop of air and water supply circuit was used for supplying two-phase flow. Flexible risers were simulated using silicon hoses. Silicon hoses provided the needed flexibility for showing dynamic responses relative to internal two-phase flows.

2. Experimental Apparatus

Air and water were supplied through the mini-loop instrumentation box shown in figure (3.1). Air was supplied using a reciprocating air compressor while water supplied through centrifugal pump.

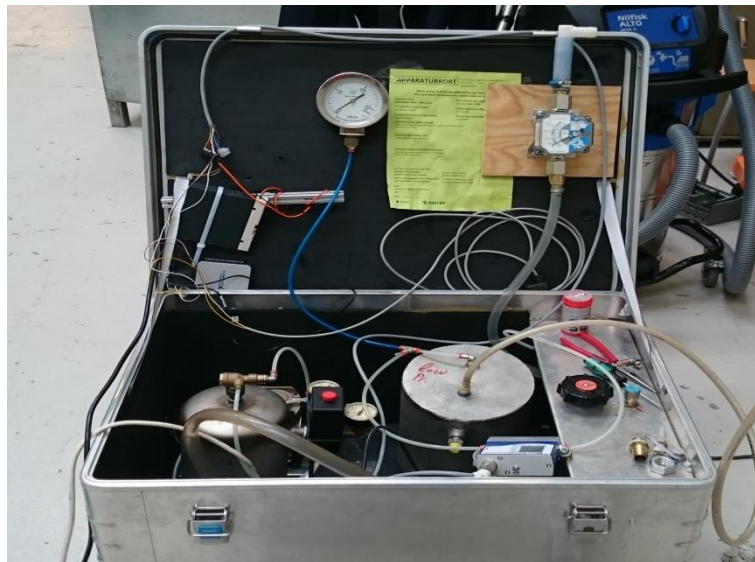


Figure (3. 1): Mini-loop instrumentation box

The air supply circuit includes high pressure tank connected directly to the compressor for receiving compressed air with 3 bar cut off valve. A low pressure buffer tank (volume: 0.032 m^3) was connected to the high pressure tank with digital mass flow meter in between. The mass flow meter gives a measure of the air flow rate. The air flow meter had a built in flow controller that was utilized for controlling flow rates through 4 – 20 mAmps current feed.

Figure (3.2) shows the compressor unit connected to high pressure tank.



Figure (3. 2): Compressor connected to high pressure tank

Water supply circuit includes a centrifugal pump connected to needle valve for adjusting flow rates and analog flow meter. A mixer was used upstream the geometry for mixing the two fluids and providing two-phase flow supply.

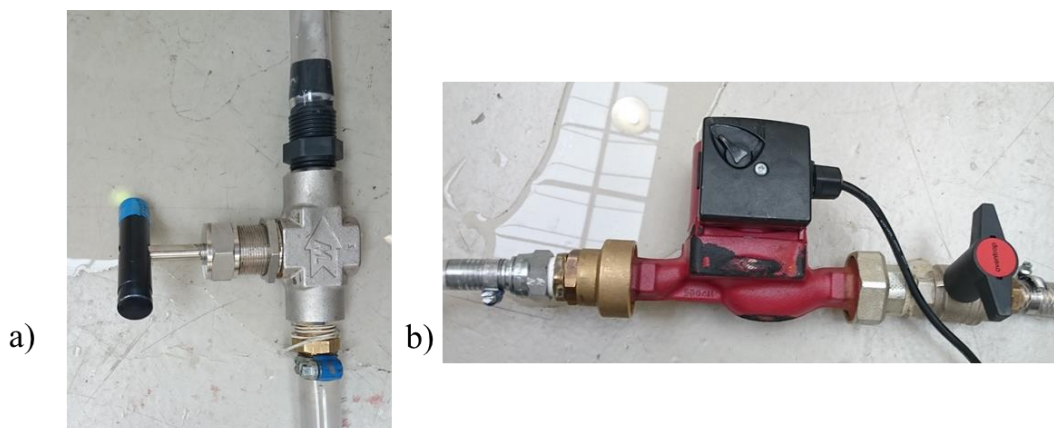


Figure (3. 3): a) Needle water adjustment valve b) Water pump

Figure (3.4) shows the schematic of instrumentation circuit used in the experiments.

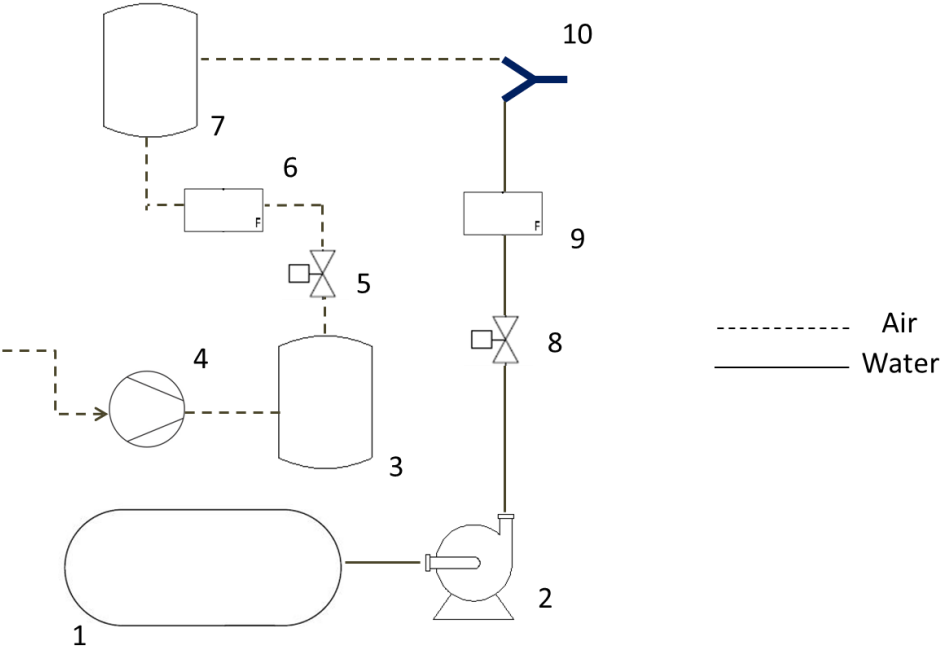


Figure (3. 4): 1- Water supply tank, 2- Centrifugal pump, 3- High pressure Tank, 4- Compressor, 5- Ball valve, 6- Digital air flow meter, 7- Low pressure buffer tank, 8- Needle valve, 9- Analog liquid flow meter, 10- Air & water mixer

Experiments were videotaped using two different cameras. A fully professional camera was used for taping the cantilever hose experiments and underwater camera used for DWH riser experiment. Table (3.1) indicates the specification of instruments used.

<i>Device:</i>	<i>Manufacturer:</i>	<i>Model:</i>
Air compressor	DING HWA	AC 100
Water pump	Grundfoss	UPS 25-40
Digital flow meter	Mass-Stream	D-D6341 DR
Analog liquid flow meter	Tec-Fluid	D-D6341 DR
Digital camera	Canon	EOS-60D
Digital underwater camera	GoPro	Hero4-black

Table (3.1): Devices used in cantilever hose experiment

2.1 – Cantilever experimental geometries

A hose arranged in a cantilever position conveying two phase flow was used for investigating the structural dynamic behavior induced by internal flow. The geometry has been investigated in both vertical and horizontal arrangements. The hose was fixed at one terminal and the other terminal was left free. Air and water were supplied through the hose.

Figure (3.5) shows the vertical and horizontal geometries used in the experiment.

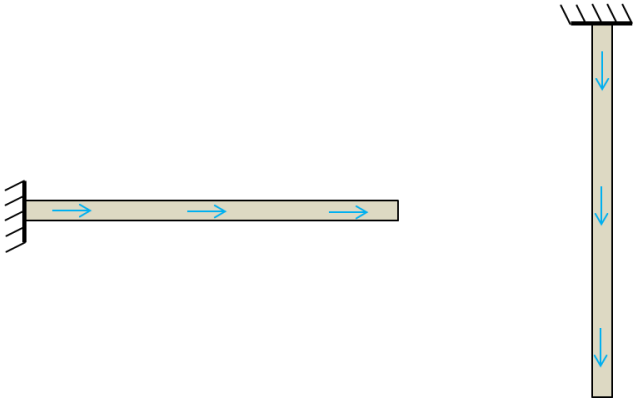


Figure (3. 5): Vertical and horizontal geometries of the cantilever hose experiments

2.2 - DWH riser experimental geometry

The geometry is reflecting the sinking of DWH drilling rig and riser extending over it at sea bed as shown in figure (1.1) before. This geometry showed a dynamic interaction between the buoyant part of the riser (part with buoyancy modules) and internal slug flow. Figure (3.6) shows the accident resulting geometry implemented in the lab.

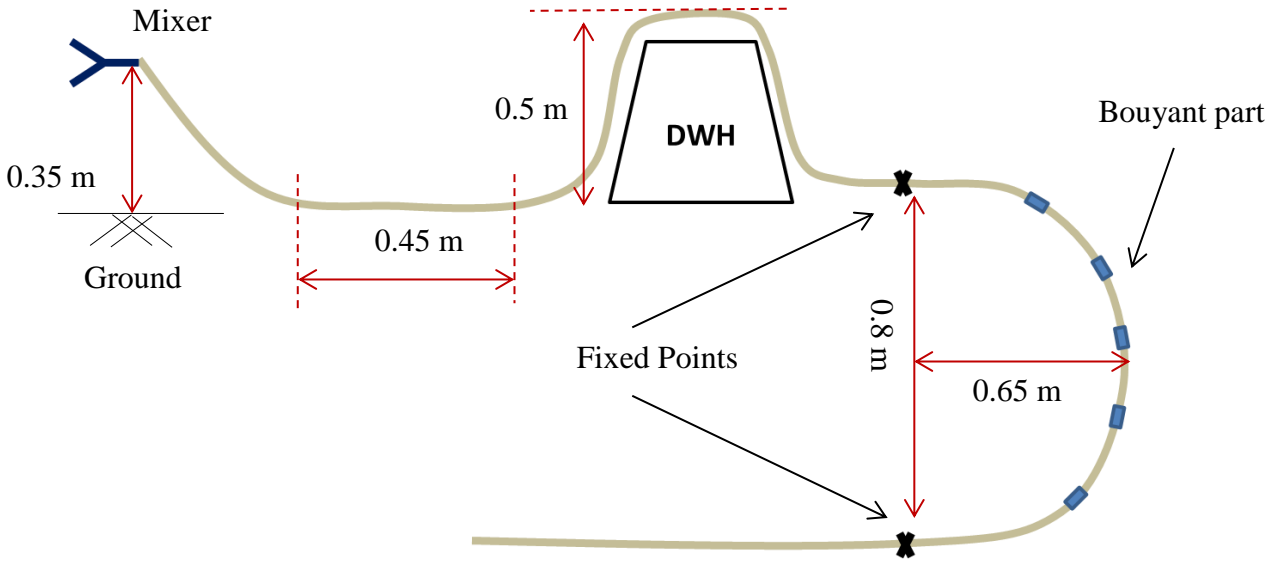


Figure (3. 6): DWH riser geometry implemented in the lab

Figure (3.7) shows the tank used in the lab where the hose was laid in. The tank was filled with water and a camera was fixed on tank bottom for taping the experiments. It is worth noting that the buoyant part needed no buoyancy modules as silicon hoses were floating on its own.



Figure (3. 7): Tank used for DWH riser experiments (0.95 x 0.95 x 0.4 meters)

Figure (3.8) shows the under-construction tank, the tank was fabricated from S.S sheets. One side will be sealed with glass plates for providing the vision.

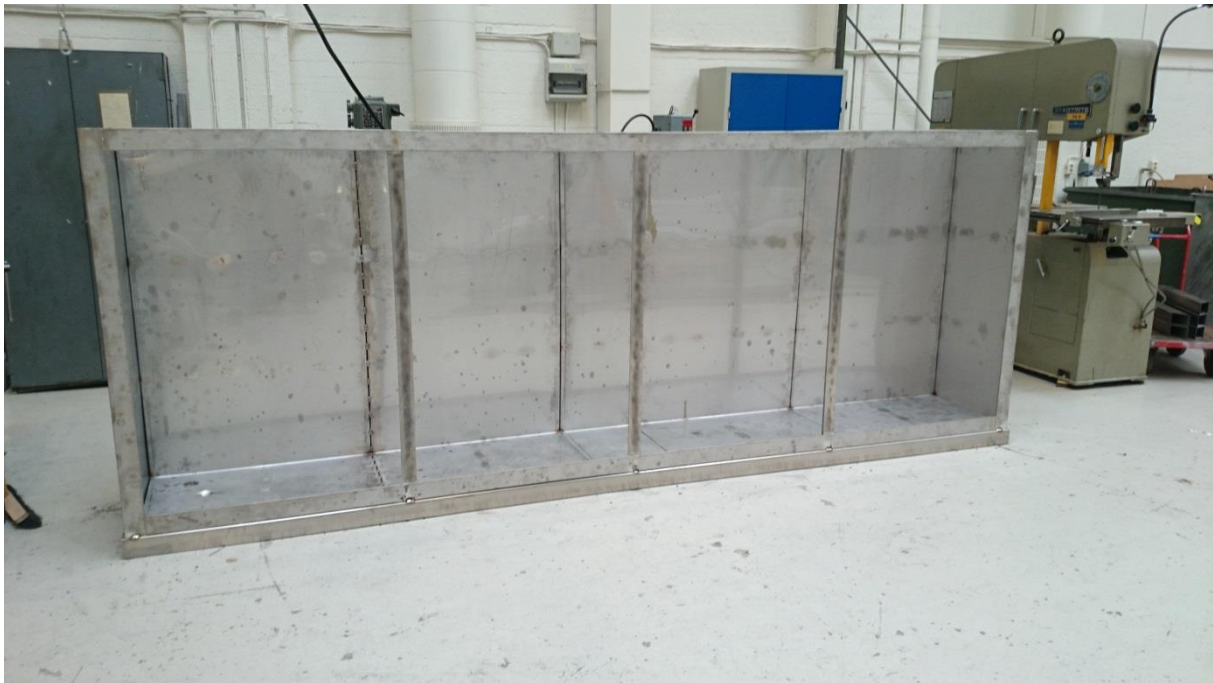


Figure (3. 8): Under-construction tank for future experiments with floating pipes, dimensions: 4 x 0.5 x 1.4 meters

3 Video Processing

The experiments were recorded and video processing techniques were used for analyzing the induced motion. A code was written in MATLAB for detecting red objects based on VideoReader class. The code works by reading saved video files from the experiments and

calculate the displacement of red detected points in vertical and horizontal directions. Figure (3.9) shows the red points detected, the displacements are measured in pixels with reference to the upper left corner of each frame as indicated by the blue arrows.

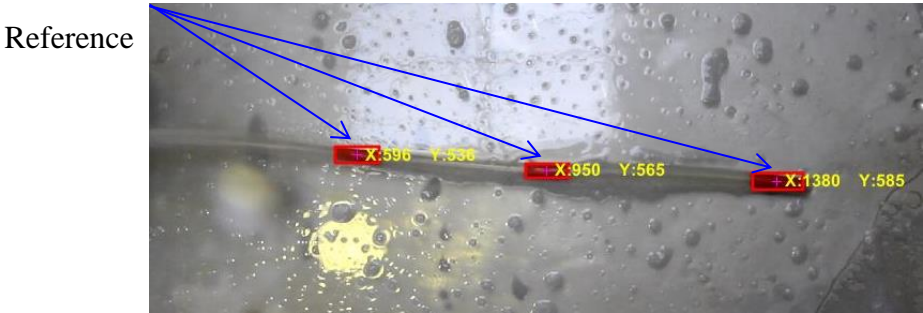


Figure (3. 9): Points detected by the MATLAB code

For converting the dimensions from pixels to cm, a scaling factor was determined by dividing the image real dimensions in cm by frame dimensions in pixels as shown in figure (3.10).

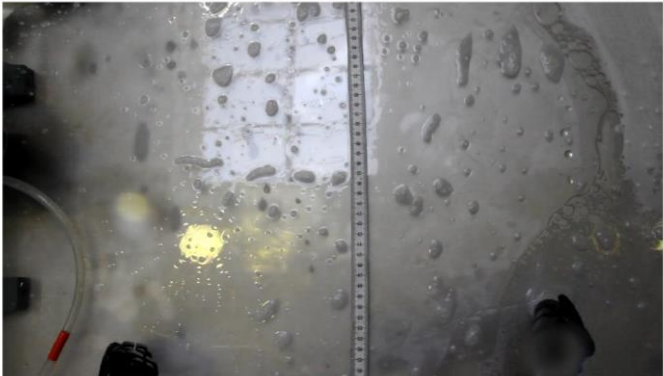


Figure (3. 10): Real scale image for experiments

4 Bending Stiffness

Two silicon hoses were used for investigating both cantilever and DWH riser experiments. The bending stiffness for the two silicon hoses used was determined by using structural dynamic analysis code described in produced scientific paper included in Appendix (A). Table (3.2) shows the dimensions and estimated bending stiffness of the two hoses.

<i>Hose:</i>	<i>Inner dia.:</i>	<i>Outer dia.:</i>	<i>Weight/Length:</i>	<i>Bending stiffness:</i>
Hose (1)	6 mm	9 mm	0.0042 Kg/m	0.001 <i>N. m²</i>
Hose (2)	16 mm	22 mm	0.189 Kg/m	0.004 <i>N. m²</i>

Table (3.2): Dimensions and bending Stiffness estimated for the two hoses

Experiments were carried out with the silicon hose allowing it to oscillate in simple harmonic pendulum motion. The hose free end was detected using the MATLAB code described before. Figure (3.11) shows how the pendulum experiment was carried out.

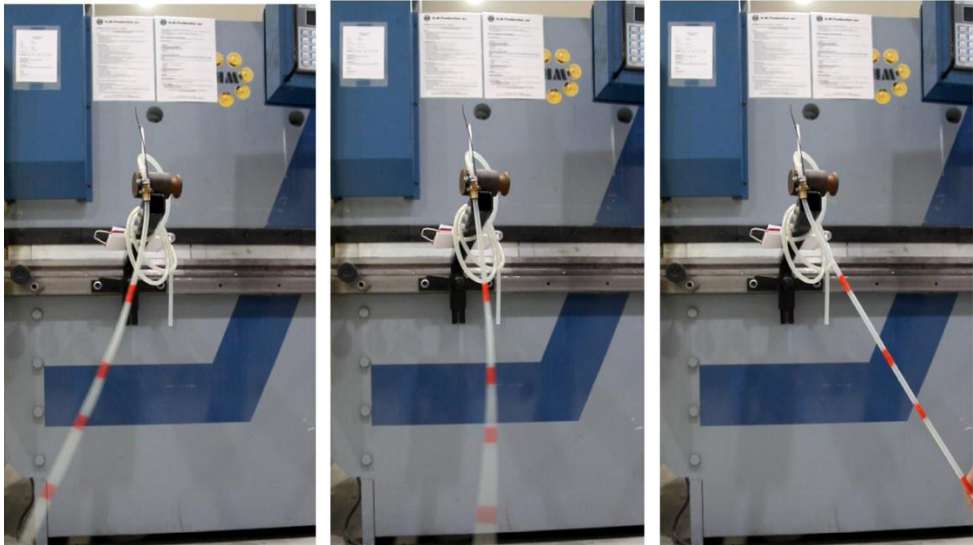


Figure (3. 11): Pendulum experiment for estimating bending stiffness

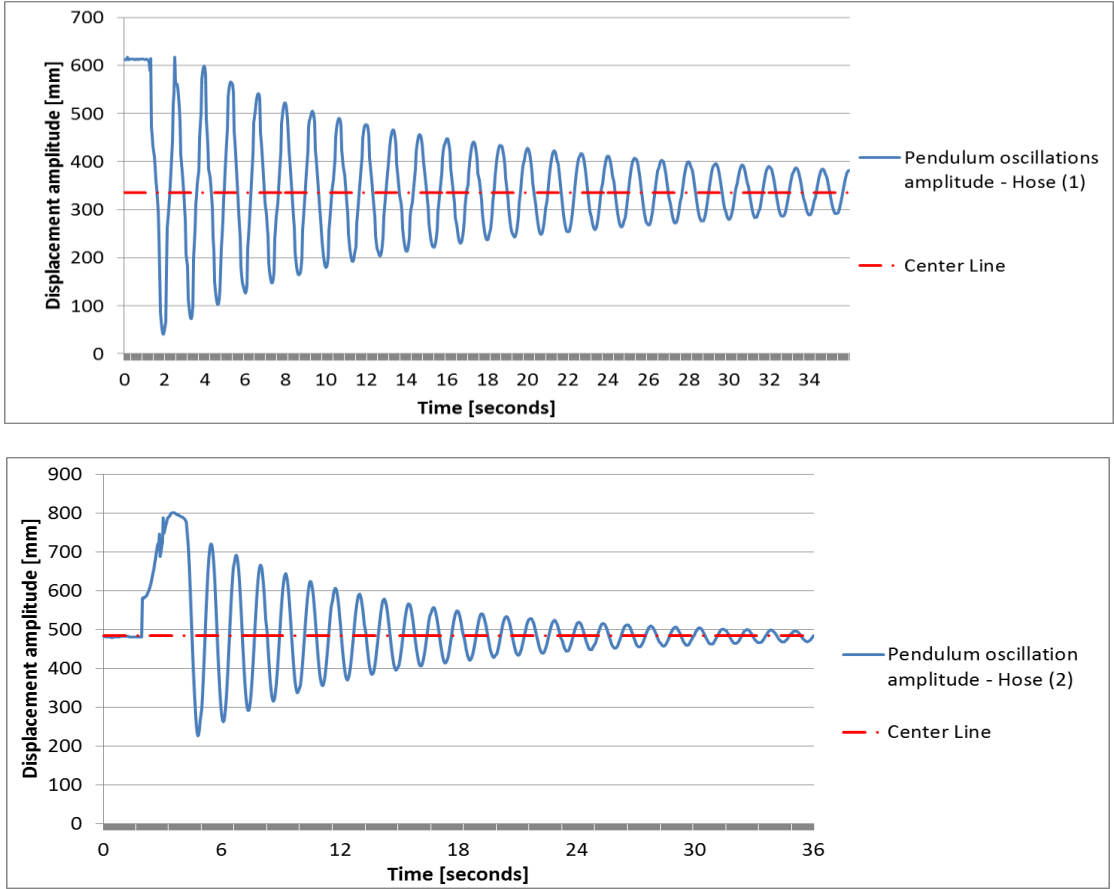


Figure (3. 12): Pendulum displacements amplitude vs. time for hoses (1) and (2)

Using the structural dynamic code, the experiment was simulated. Different values for bending stiffness and damping coefficient were tested until reaching a value that showed similar oscillation period to the experiment.

Figure (3.13) shows the amplitude per cycle for both experimental and simulation results for hose (1). It was found that a bending stiffness of 0.001 gives a satisfactorily matching result.

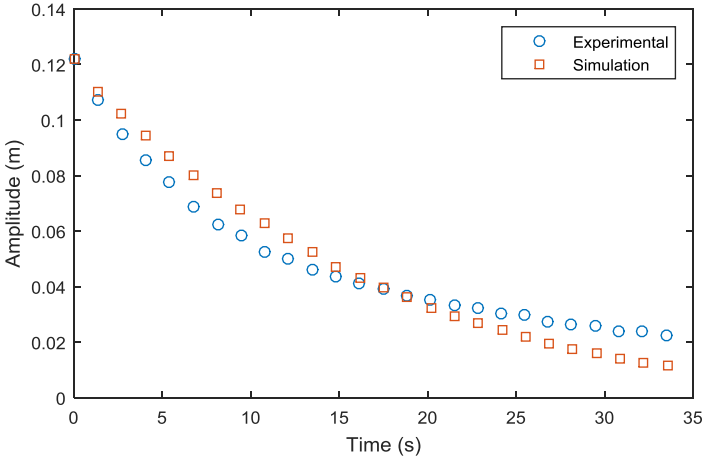


Figure (3. 13): Experimental and simulation amplitude per cycle of pendulum experiment for estimating bending stiffness of hose (1) – [10]

5 Flow Rates Measurements

The accuracy of the air and liquid flow meters used is $\pm 2\%$. The gas meter gives the reading in Liter/min while the liquid meter gives the reading in Liter/hour. In the cantilever hose, the liquid flow rates were measured by calculating the time elapsed for filling one liter of water.

The measurements were taken from the oscillating hose directly with gas and liquid flowing together. In DWH riser experiments, the liquid flow meter was available and readings were measured directly from the meter before the air & water mixer. Results are presented relative to gas and liquid superficial velocities.

Superficial velocity is defined as the phase volume flow divided by pipe cross sectional area according to equation (3.1). [5]

$$U_{sk} = \frac{Q_k}{A} \dots\dots (3.1), \text{ where } Q_k \text{ is the flow rate measured from the flow meter in } [m^3/s].$$

The inaccuracy (Ω) in flow meter results in an uncertainty in measured flow rates which creates an error propagating in calculated superficial velocities. The resulting error propagation can be expressed by the following equation;

$\frac{\sigma_{U_{sk}}}{|U_{sk}|} = \sqrt{\left(\frac{\Omega}{Q_k}\right)^2}$ (3.2), where $\sigma_{U_{sk}}$ represents the error propagating in the superficial velocity calculated. [11]

Chapter (4): Cantilever Hose Experiments

Both horizontal and vertical geometries were investigated at several cases of different gas and liquid superficial velocities and different lengths. The two geometries were tested with single phase flow but showed no any dynamic response.

1. Horizontal Geometry

The hose was fixed at one terminal with other terminal free to oscillate. Several points marked by red tape were detected during the videotaped experiments. With the maximum length of 71 cm, five points were selected with Point (1) as first point after fixed end. Figure (4.1) shows distances [cm] in which points were placed with reference to fixed end.

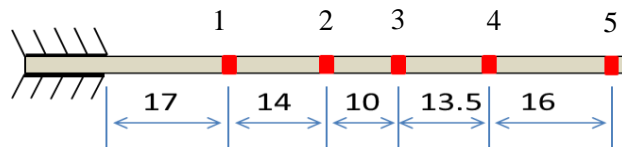


Figure (4. 1): Red detected point's distances from fixed terminal

At very low velocities, no oscillations in the hose were observed. The hose started oscillating at approximately 4.42 m/s of air flowrate and 0.355 m/s of water. Table (4.1) summarizes the cases where experiments were carried out.

<i>Case no.</i>	<i>U_{sg} [m/s]</i>	<i>U_{sl} [m/s]</i>	<i>Length [m]</i>	<i>Inner Φ [m]</i>	<i>Outer Φ [m]</i>
(1)	6.77	0.584	0.71	0.006	0.009
(2)	6.77	0.523	0.71	0.006	0.009
(3)	6.77	0.355	0.71	0.006	0.009
(4)	3.53	0.584	0.71	0.006	0.009
(5)	6.77	0.584	0.5	0.006	0.009

Table (4.1): Summary of cases tested for horizontal experiment

Figure (4.2) shows oscillations trajectory for the 5 points in both vertical and horizontal directions for case (1). The figure shows that moving from point (1) to point (5); it can be observed that a rotational motion pattern increases. As expected, more close to the fixed point

the motion is less rotational with no large changes in the horizontal displacements. The stroke traveled by every point is indicated by the dotted arrows. That is the maximum distance travelled by the every point across the centerline reaching maximum displacement above or below centerline.

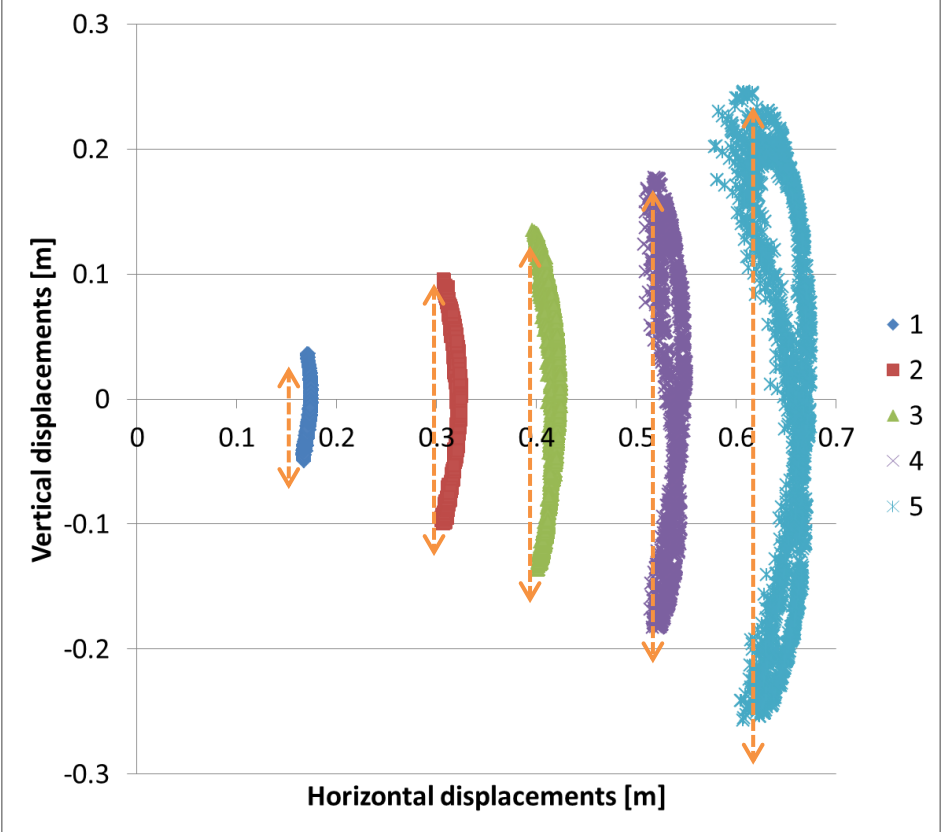


Figure (4. 2): Trajectory of all point’s oscillation displacement in both vertical and horizontal directions for case (1)

Figure (4.3) shows the number of strokes traveled by point (5) vertically over a two minutes length of the video. The figure shows about 8 peaks and 7 troughs across center line corresponding to about 15 strokes travelled by point (5) over two minutes.

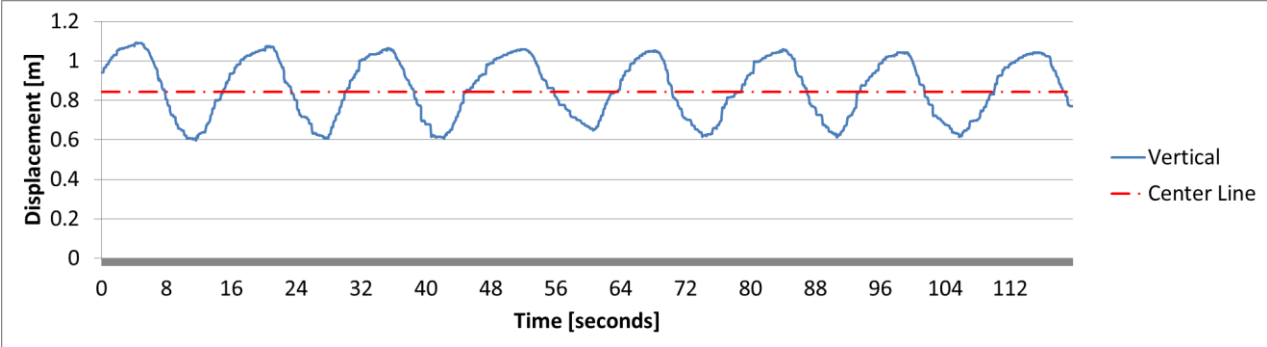


Figure (4. 3): Number of strokes travelled by point (5) for case (1) with reference to upper left corner of every frame of the video

The center line is the line where the hose is extending symmetrically in straight position when subjected to no flow (X-axis in figure (4.2)). The stroke's displacement is referenced to the upper left corner of the video frame.

Figure (4.4) shows the relation between the maximum vertical and horizontal displacements of each detected point and its distance from the fixed point. The figure shows that points (4) and (5) are deviating more from the line due to their rotational movement.

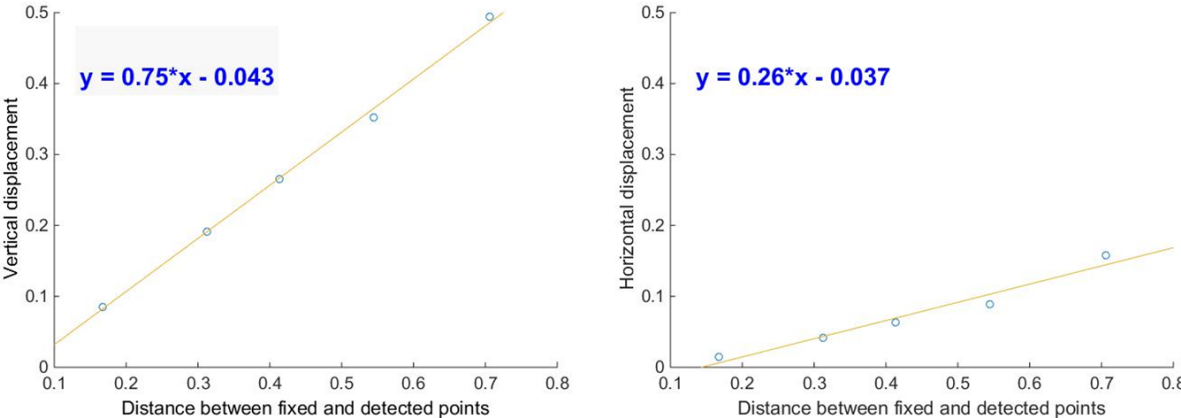


Figure (4. 4): The relation between vertical and horizontal displacements of points (1) to (5) relative to distance of each detected point from fixed one

The trajectory of points (1), (2) and (3) shows motion pattern that can form an ellipse if the hose was rotating 360 ° with fixed point as center of rotation. The ellipse shape is due to the flexibility of the hose, if a rigid pipe was to be used, the motion would tend to show a perfect circle. Points (4) and (5) have more rotational oscillating motion that cannot form a perfect ellipse as the first three points. Figure (4.5) shows the ellipse motion pattern formed by the first three points.

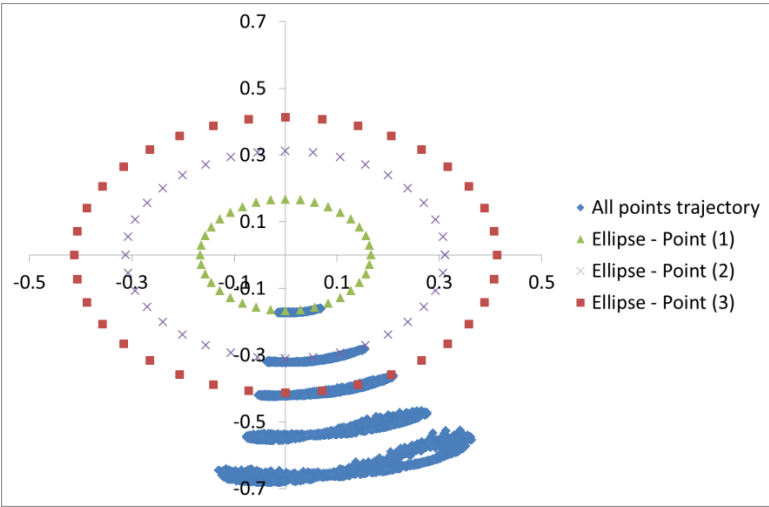


Figure (4. 5): Ellipse motion pattern made by points (1), (2) and (3)

Two frequencies were noted during the experiments. First, is the total stroke travelled by the hose as shown before, second are small perturbations relative to the alternating liquid and gas flows.

These small perturbations are responsible for step movement of the hose that continues until the hose travels a full stroke. Every time a liquid slug is flowing out the hose free end is displaced by small amplitude. Figure (4.6) shows the perturbations caused by liquid slugs, it can be seen from figure that the slug frequency is approximately 3 slugs per second.

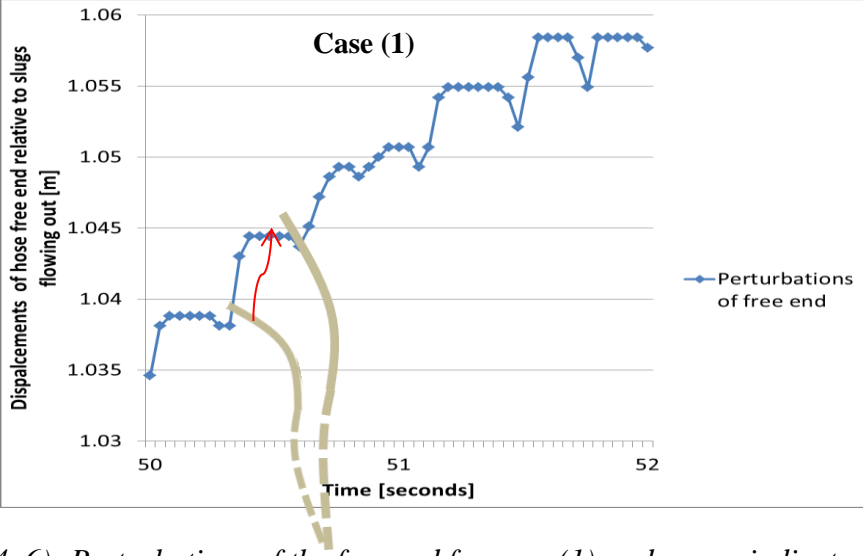


Figure (4. 6): Perturbations of the free end for case (1), red arrow indicates distance displaced by the hose due to liquid slug flowing out

When liquid superficial velocity was reduced in cases (2) and (3), the perturbations amplitude was less compared to case (1). This reduction of amplitude is an indication of shorter liquid slug with lower flow rates. Figure (4.7) shows the perturbations for cases (2) and (3), it can be seen how the curve became smoother with less perturbation amplitudes.

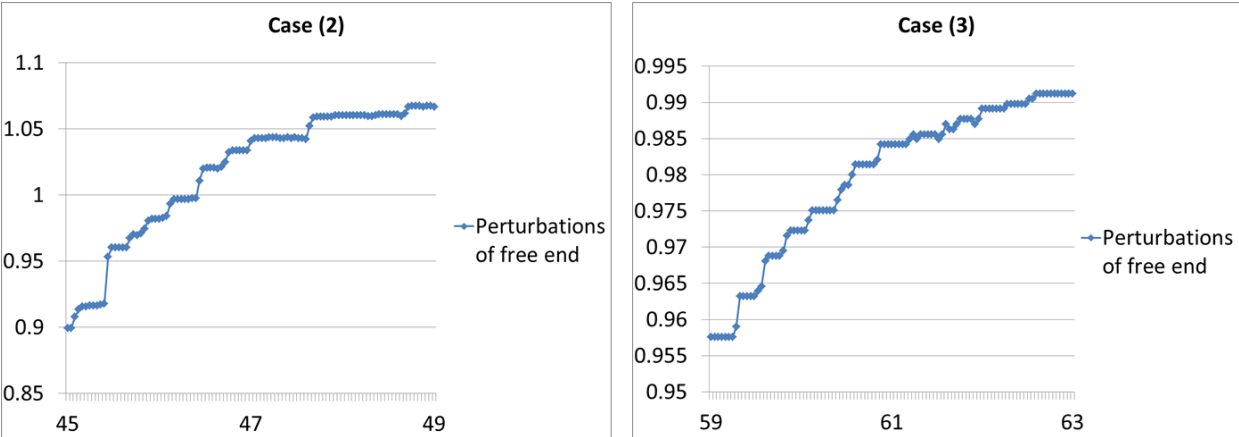


Figure (4. 7): Perturbations of hose free end for cases (2) and (3); the curve is smoother indicating shorter step displacement for the perturbations

The results of case (2) and (3) showed little change in the amplitude of stroke travelled by every point. The motion trajectory was also same as shown in Figure (4.2) before. However, it was noted that the motion was getting significantly slower with reducing the liquid superficial velocity. This resulted in less number of strokes travelled by detected points in the two cases. Figure (4.8) shows the strokes travelled by point (5) for the three cases.

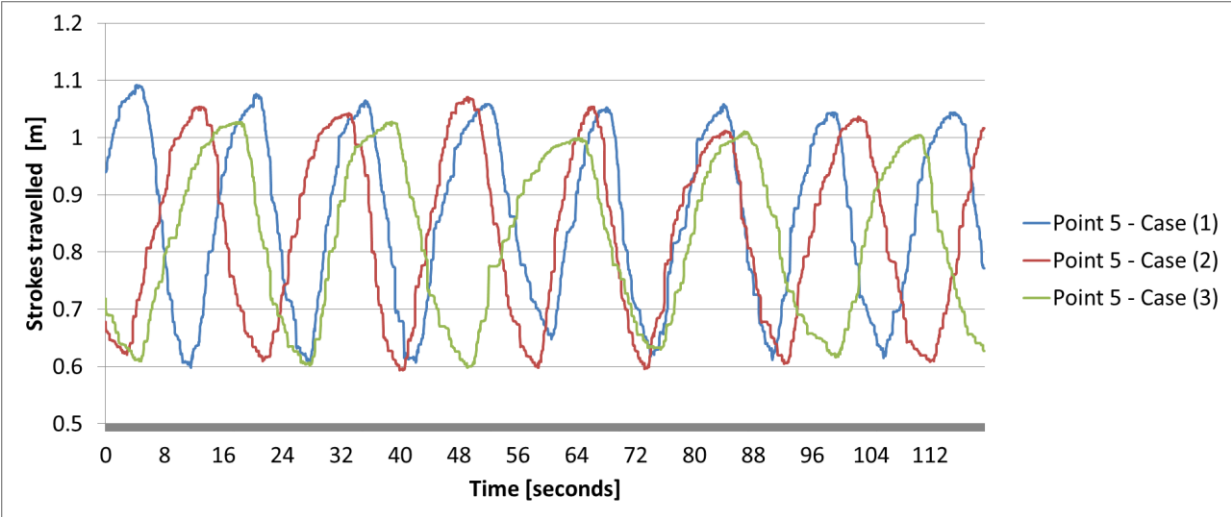


Figure (4. 8): Strokes travelled by point (5) for cases (1), (2) and (3)

In case (4), there was no oscillation when the hose was kept at center line (symmetric position). However, when it was positioned in maximum displacement from centerline, the hose started oscillating moving towards the center line until stopped oscillating. In other words, the hose travelled only half stroke from maximum displacement until center line as shown in figure (4.9).

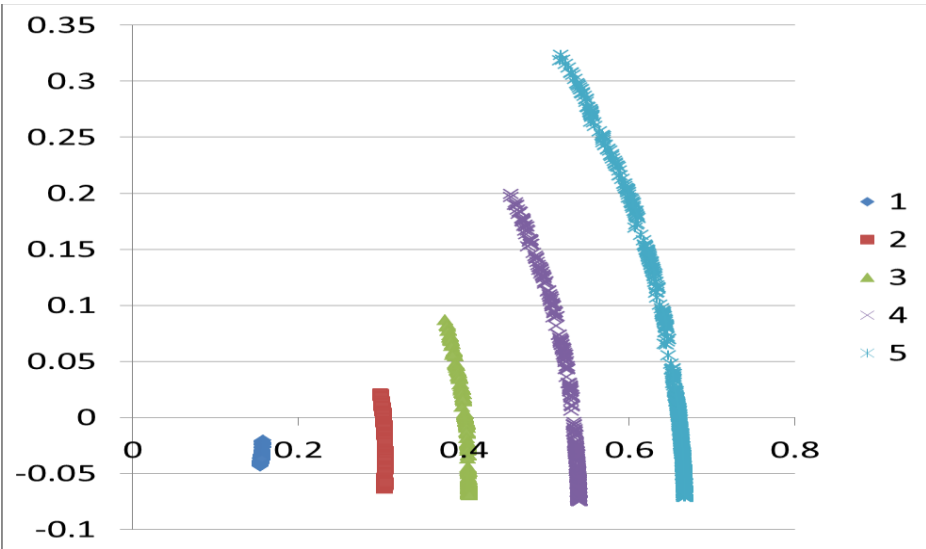


Figure (4. 9): Trajectory of half stroke travelled by points in case (4)

In case (5), the effect of length was studied by reducing the length of the hose to 50 cm and studying the three points (3), (4) and (5). With maximum superficial velocities the hose showed no oscillations. Instead the hose showed only vibrations while lying in symmetric position on the center line. Figure (4.10) shows the vibrations measured in [mm].

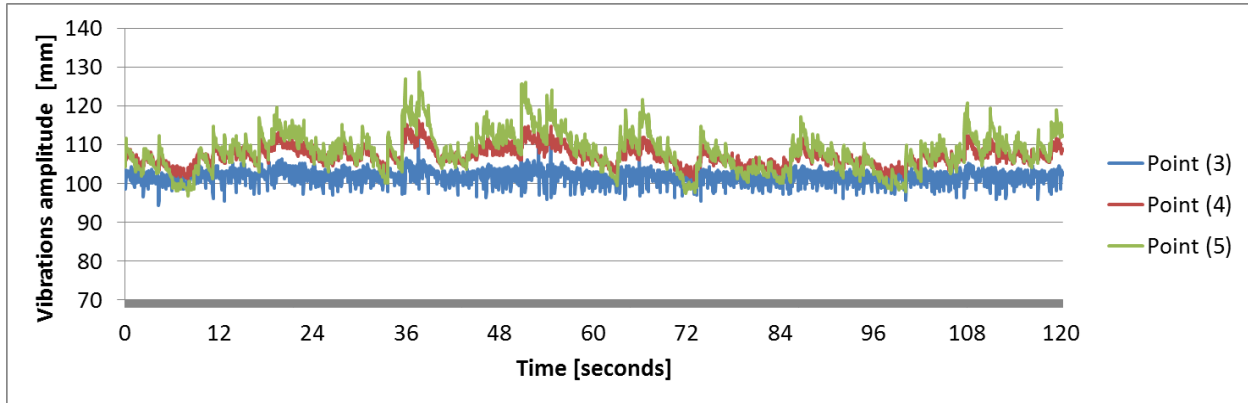


Figure (4. 10): Vibrations of points (3), (4) and (5) for case (5) with 50 cm length of hose

2. Vertical Geometry

The vertical geometry was tested with two-phase flow at high gas and liquid superficial velocities. The hose showed only slight vibrations at high velocities and therefore lower velocities were not considered.

Three cases were studied for investigating the effect of length change. Table (4.2) shows the cases studied for this geometry.

<i>Case no.</i>	<i>U_{sg} [m/s]</i>	<i>U_{sl} [m/s]</i>	<i>Length [m]</i>	<i>Inner Φ [m]</i>	<i>Outer Φ [m]</i>
(1)	6.77	0.584	0.90	0.006	0.009
(2)	6.77	0.584	0.70	0.006	0.009
(3)	6.77	0.584	0.50	0.006	0.009

Table (4.2): Study cases for vertical geometry

As the hose was slightly vibrating at the free end, only one point was detected for measuring the dynamic behavior of the vertical hose as shown in figure (4.11).

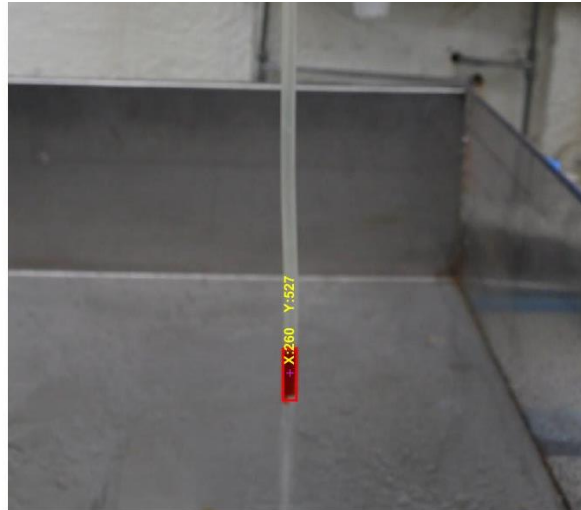


Figure (4. 11): Hose free end detected point

The vibrations of end point are shown in Figure (4.12). Unlike the horizontal cases, the vertical hose cases showed an increase in amplitude of vibrations as the length reduces. The average amplitude of vibrations at 50 cm is slightly larger than 70 cm. However, in case of 90 cm the vibrations amplitude has dropped significantly as seen in the figure.

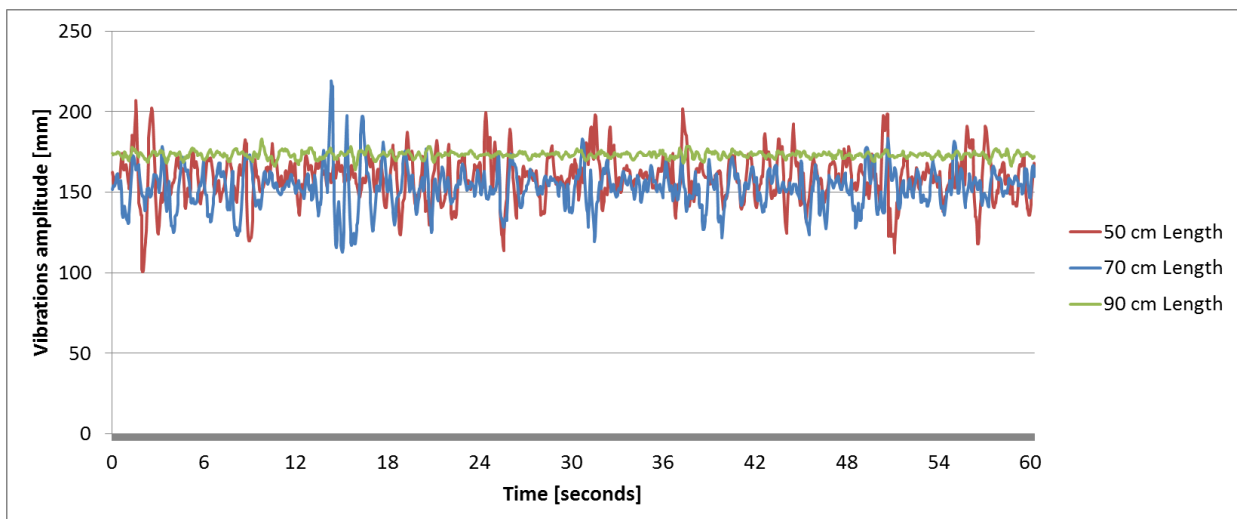


Figure (4. 12): Vibrations amplitude for cases (1), (2) and (3) of vertical geometry

3. Discussion

The experimental results showed that liquid flow rates have an effect on oscillating speed and therefore number of strokes travelled. Momentum of liquid slugs gives the small perturbations shown in figure (4.6) before. The liquid slug travels at mixture velocity where mixture velocity is the sum of gas and liquid superficial velocities ($U_m = U_{sl} + U_{sg}$).

Since the gas flow rates are higher compared to liquid flow rates, the mixture velocity would be dominated by gas superficial velocity ' U_{sg}' '. This explains the reason behind having little change in amplitude of oscillations in the experiments at different liquid flow rates. Increasing liquid superficial velocity ' U_{sl}' increases the slug fraction resulting in larger displacement by slug perturbations and therefore faster oscillations.

The paper produced in appendix (A) explains in details the coupling between experimental data and structural dynamic simulations. Figure (4.13) demonstrates the trajectory of simulation and experimental results for case (1).

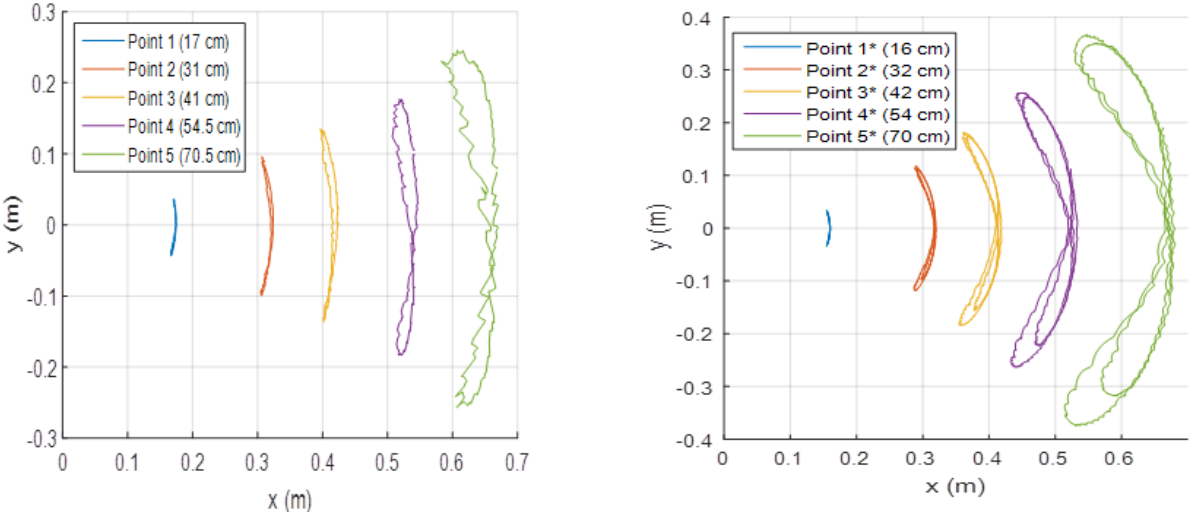


Figure (4. 13): Trajectory of experimental and simulation results for case (1)

Compared to experimental, the figure shows similarity in both simulation and experiments oscillation pattern. The rotational motion of the last two points was observed in simulations as in experiments.

Chapter (5): DWH Riser

Small scale experiments were conducted for demonstrating the physics behind structural behavior of the DWH riser in small scale experimental apparatus in the lab. The experimental results are compared to simulations and discussed in this chapter.

1. DWH Riser Case Description

After the DWH drilling rig sank to the sea bottom, the riser was extending over the rig forming the geometry shown before in figure (1.1). The buoyant loop was oscillating between two positions, resting on the seabed and floating above seabed. The following steps explain the cyclic motion mechanism.

- 1- As the buoyant loop is in its highest floating position, gas flows over the oil with higher velocity due to density difference. Gravity has stronger effect on oil being the denser fluid, holding oil back where oil starts accumulating at the bend as shown in figure (5.1).

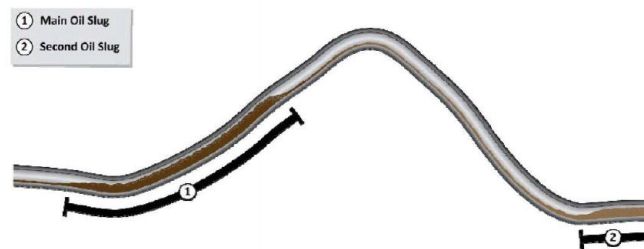


Figure (5. 1): Main oil slug accumulating in upstream section of buoyant loop [4]

- 2- Oil accumulation increases approaching the top of the buoyant. As the upstream part of the buoyant loop gets heavier it starts pushing the loop towards the seabed.

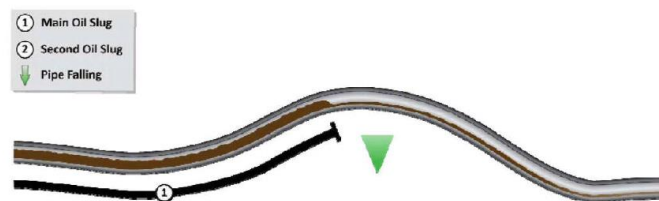


Figure (5. 2): Oil flowing towards top pushing the buoyant loop to sink towards seabed [4]

- 3- The oil slug moving through the loop is followed by stratified flow pattern. The loop at this stage is resting on the seabed as shown in figure (5.3).

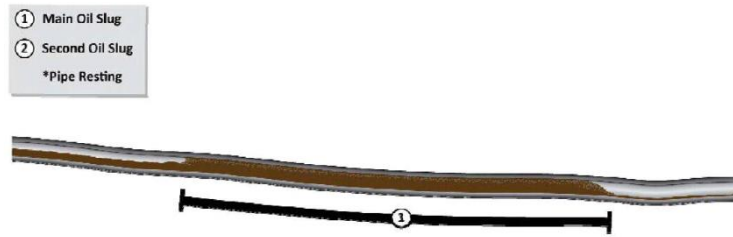


Figure (5. 3): Buoyant loop resting on seabed and stratified flow pattern emerges [4]

- 4- After oil completely passes the top of the buoyant loop, the upstream section of the buoyant loop with gas dominated flow starts rising again as it gets lighter and lighter. [4]

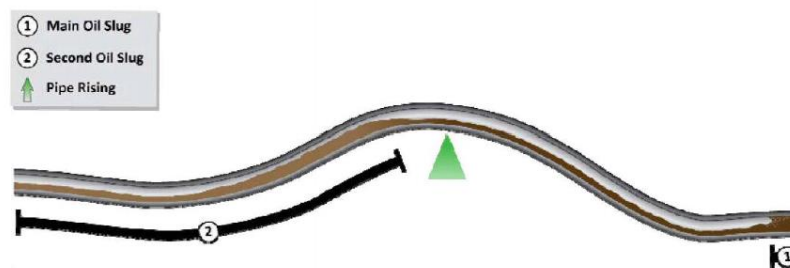


Figure (5. 4): Buoyant loop rising again after filling with gas [4]

1.1 – Double and single peak pattern

Two behaviors were observed for the DWH riser flow output. Between May 13 and May 15, two sets of gas dominated and oil dominated flow periods existed.

This double peak behavior can be seen in Figure (5.5) with a pattern of two peaks and two troughs. On May 16 the double peak pattern disappeared and flow consisted of one gas dominated and one oil dominated flow per slug period. This was recognized as single peak behavior. [4]

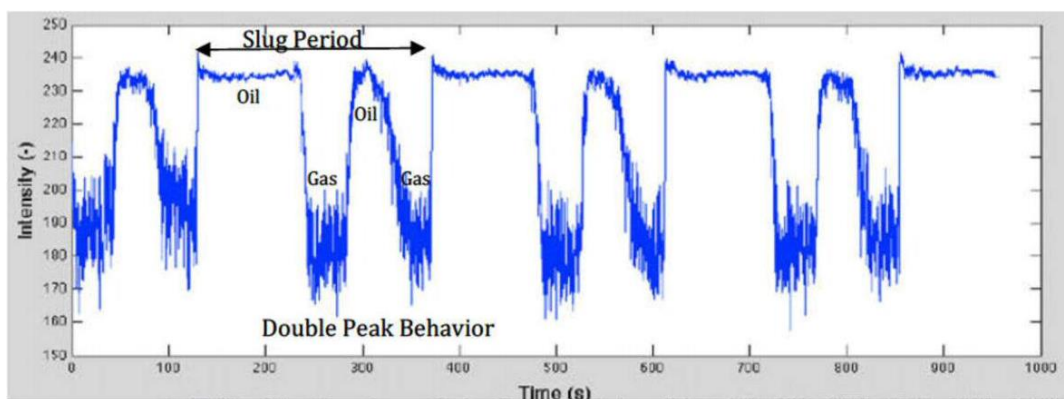


Figure (5. 5): Double peak behavior for flow output [4]

When the buoyant loop was floating on maximum distance from seabed, stratified gas and liquid flow existed. The stratified oil layer closer to the buoyant loop middle top (peak) was flowing through less steep section compared to the layer flowing at the bottom.

The oil climbing through the steepest part is slowed by gravity allowing a gas pocket to form above it. The stratified flow has in fact split into two oil slugs separated by a gas pocket as shown in figure (5.6). This explains the double peak behavior observed from May 13th to May 15th.

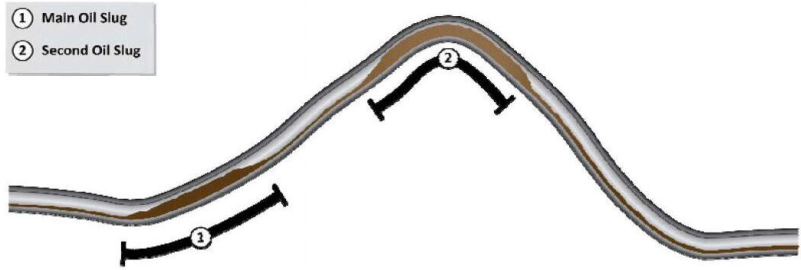


Figure (5. 6): Stratified flow splitting into two oil slugs – double peak behavior

2. Experimental and simulation results

The experiments aimed at investigating slug period, amplitude of riser down motion and flow regimes. Table (5.1) shows the different gas and liquid superficial velocities for every case. A larger silicon hose was used for this experiment as the smaller diameter hose used in cantilever hose experiments did not show expected slugging behavior.

Case no.	U_{sg} [m/s]	U_{sl} [m/s]	Inner \varnothing [m]	Outer \varnothing [m]
(1)	0.058	0.055	0.016	0.022
(2)	0.058	0.138	0.016	0.022
(3)	0.116	0.055	0.016	0.022
(4)	0.116	0.138	0.016	0.022

Table (5.1): Study cases for DWH riser experiment

2.1 – Case (1)

Figure (5.7) shows how liquid filling takes place as the liquid accumulation starts growing climbing the riser until reaching the middle point in the buoyant loop indicated by blue arrow. The figure demonstrates how the liquid weight affects the movement of the riser and pushing

it down towards tank bottom as in DWH case. The deepest displacement for the riser is when the liquid passes the middle point (indicated by blue cross).

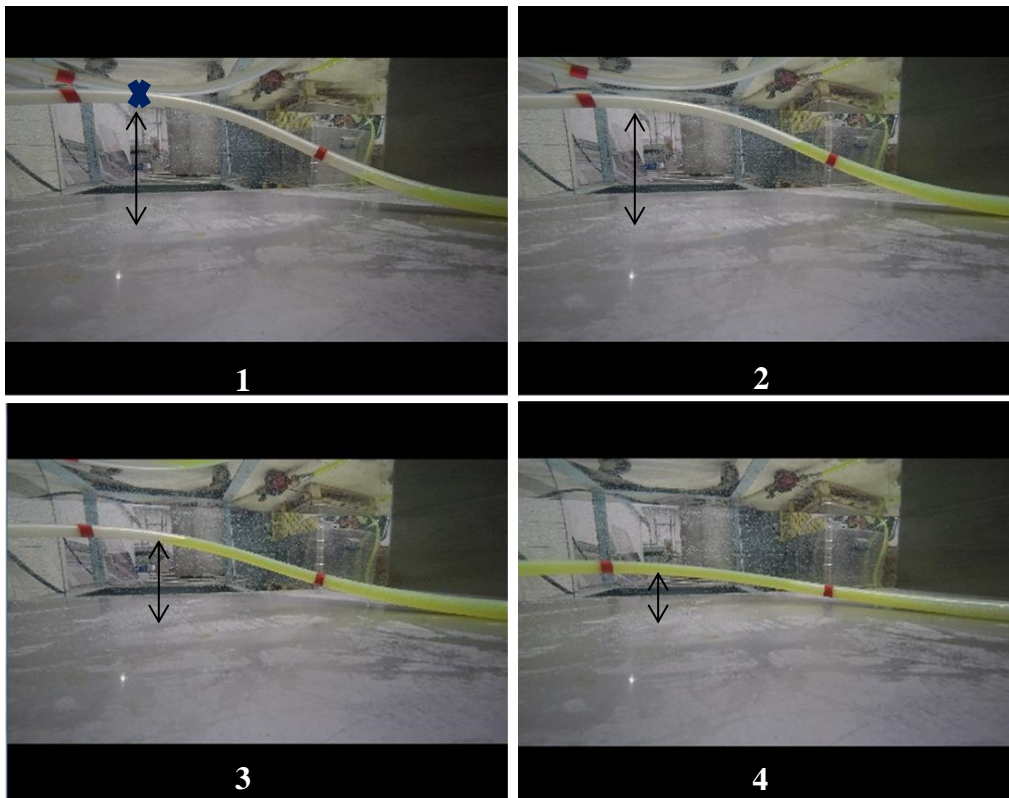


Figure (5. 7): Liquid filling buoyant loop for case (1)

The flow upstream the buoyant loop and before the liquid filling stage was gas dominant. This can be shown in Figure (5.8); the flow regime observed was stratified flow. However, the gas layer gets shorter when coming closer to the buoyant loop until forming an elongated bubble shape. When the buoyant loop is floating on water surface, the gas bubbles continue to flow while the liquid being more dense fluid stops at the bend and starts accumulating.

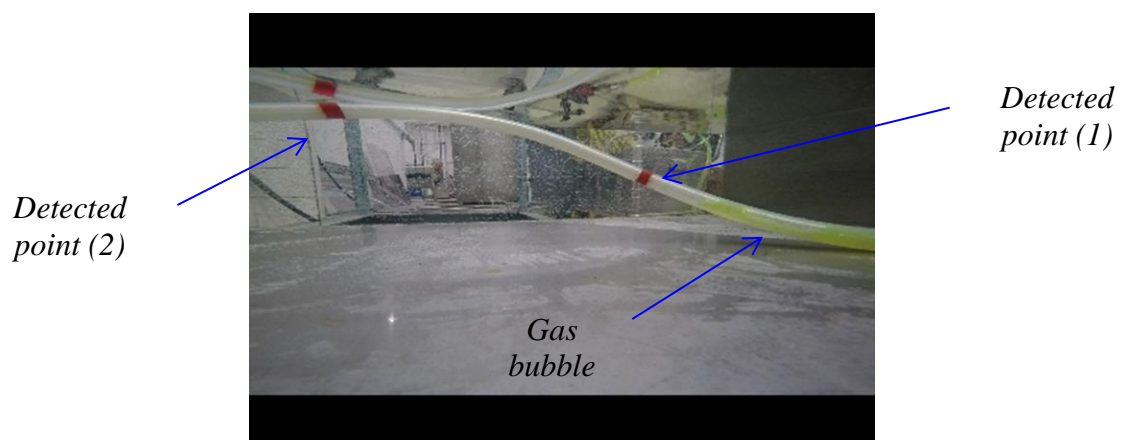


Figure (5. 8): Elongated bubbly flow prior to liquid accumulation

After liquid accumulates, it starts rising up the buoyant loop until passing over top middle point. At this stage the buoyant loop is lying on tank bottom. Once the liquid slug passes the second red detected point, a stratified flow regime starts upstream the buoyant loop as shown in figure (5.9).

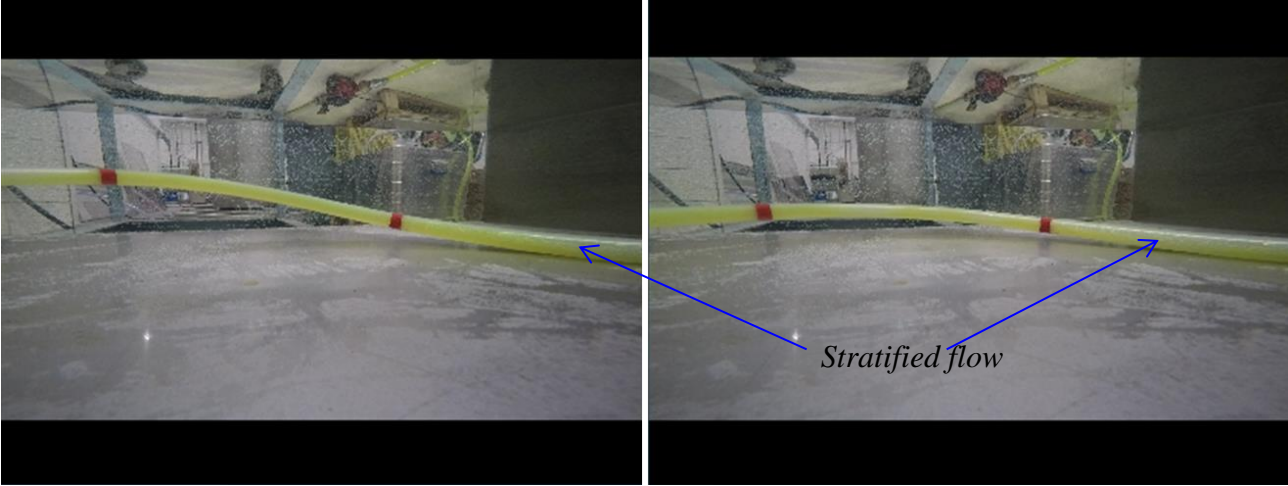


Figure (5. 9): Stratified flow starting after liquid accumulation

Figure (5.10) shows the development of slugging cyclic behavior for the experiment through the two detected points. As point (2) is closer to the top middle point of the buoyant loop it experienced the largest displacement.

The troughs shown in the graph are indication where the riser was pushed down to the deepest position by liquid slug. The flat peaks indicate the period where the flow was gas dominated and riser is floating on water surface. The displacements are referenced to lower left corner in DWH experiments to match the simulations plots. The figure shows approximately four slug periods during a two minutes time scale.

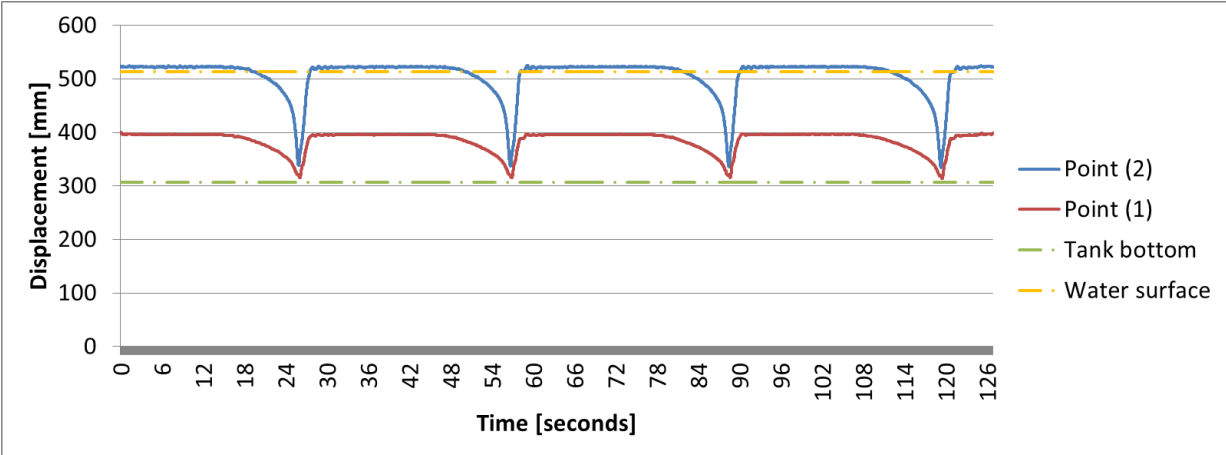


Figure (5. 10): Slugging behavior for case (1)

Figure (5.11) shows in details the liquid filling stage. It can be seen that the time for liquid slug to continue filling the hose until passing the top middle point is approximately 20 seconds (between 16 and 26 on time scale). At 26 seconds the riser starts to be dominated by gas and floats up to the water surface.

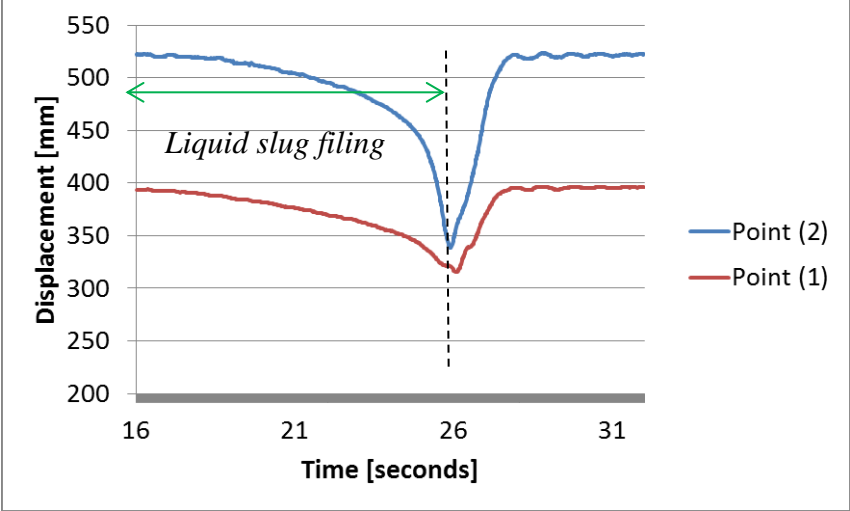


Figure (5. 11): Liquid slug filling up the buoyant part and pushing it down towards tank bottom

Figure (5.12) shows the simulation result for case (1), the figure shows a satisfactory matching result with the experiment. During two minutes time scale the simulation showed about five slug periods.

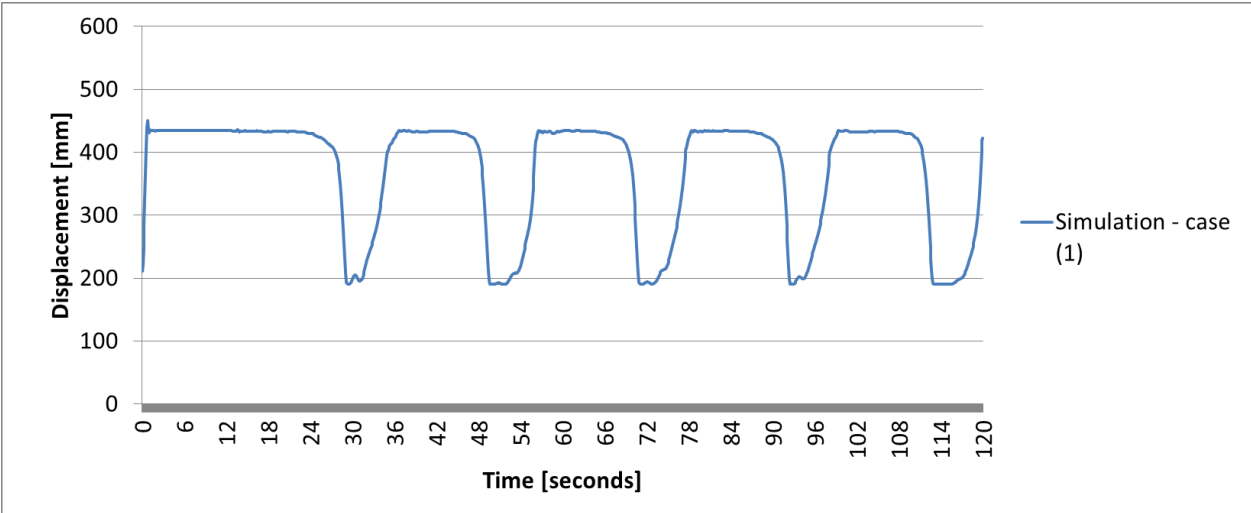


Figure (5. 12): Displacements of simulation results for case (1) over two minutes [19]

2.2 – Case (2)

Figure (5.13) shows the slugging behavior for case (2), it is obvious the cyclic behavior have taken a slightly different pattern. Now the buoyant loop stays longer in the tank bottom for about 10 seconds. The behavior is more dynamic with 6 liquid filling stages. The inclination for liquid filling is steeper compared to case (1) indicating less time for liquid filling. The figure also shows a pointed part at every trough.

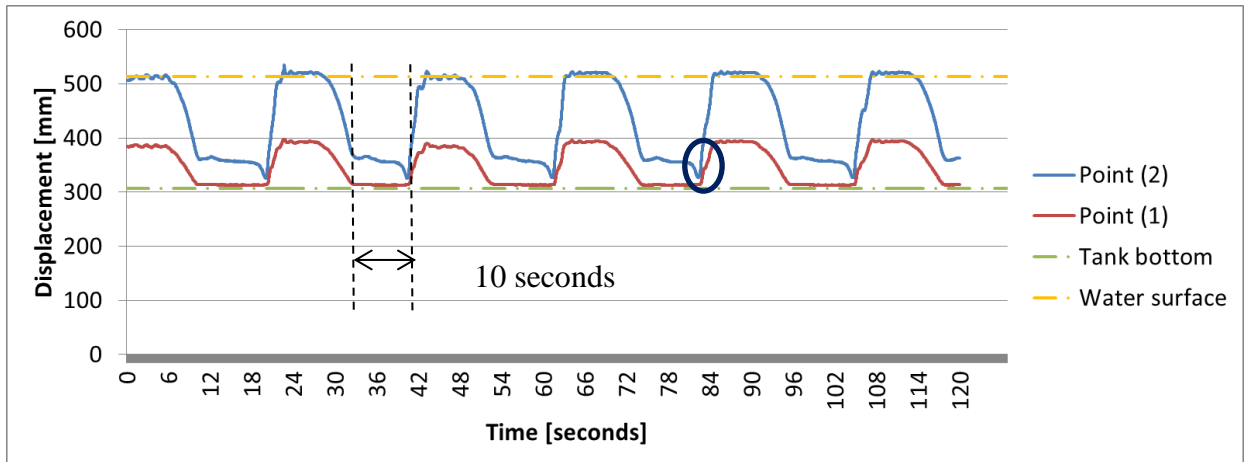


Figure (5. 13): Slugging behavior for case (2) showing flat troughs with small pointed part

Reviewing the videos, it was noted that the riser is pushed to a deep level while water in flowing over point (1). After passing over point (2) the riser is pushed further till the bottom before rising up again by air flow. This is the motion indicated by pointed arrow shown in the figure above, the images in figure (5.14) shows this motion.

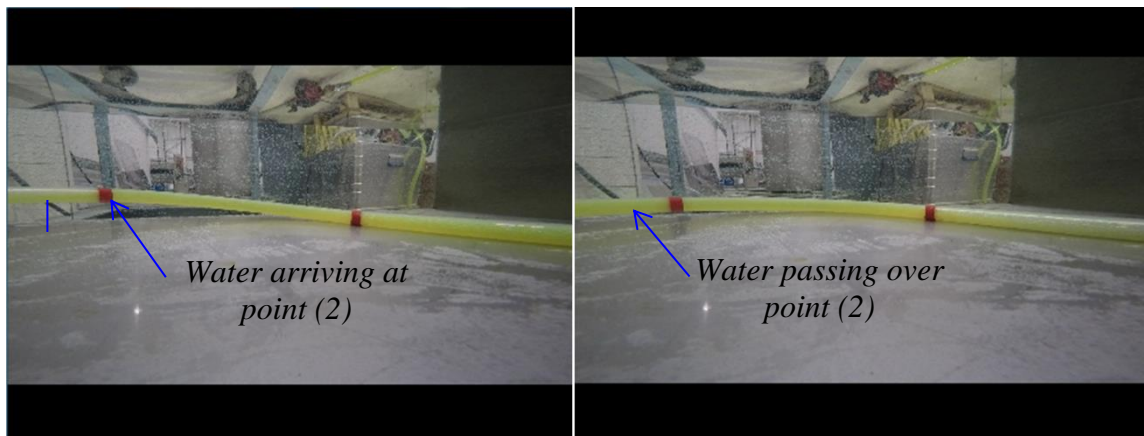


Figure (5. 14): Left image shows slug filling until point (2), right image shows slug passed point (2) pushing the buoyant loop to a lower depth

Figure (5.15) shows the simulation results for case (2). It can be observed that the motion pattern is not very similar to the experiments. However the figure shows that the number of

displacements increased compared to case (1) simulations. This agrees with the experimental results of the two cases.

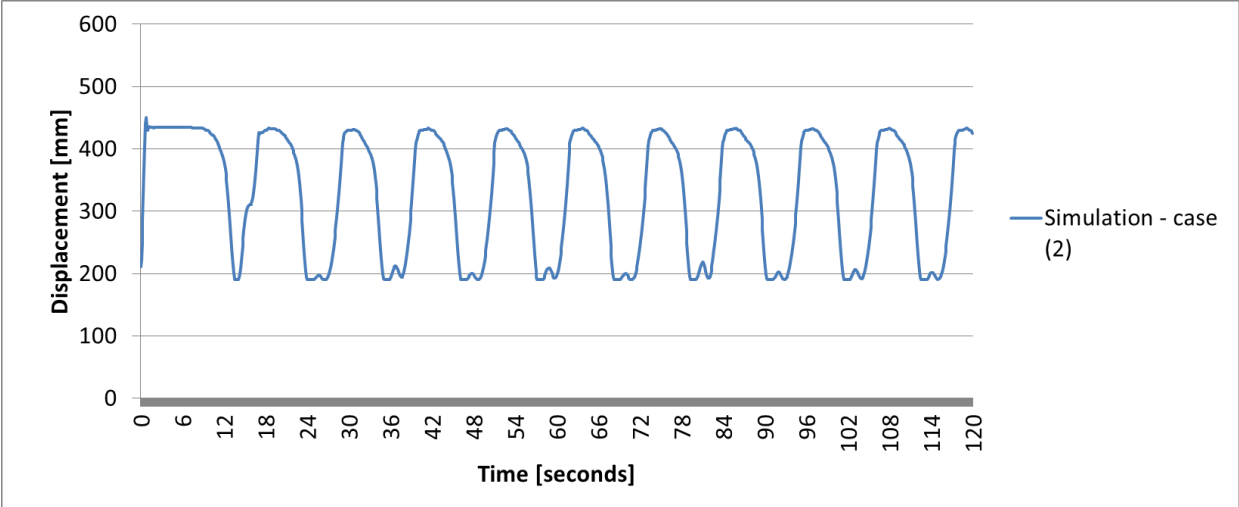


Figure (5. 15): Simulation results for case (2) with increased no. of displacements [19]

2.3 – Case (3)

The experiment showed less displacement compared to previous cases as seen in figure (5.16). The figure shows about 5 displacements per minute. Liquid filling takes less time compared to previous two cases. It is worth noting that the oscillation in this case is less uniform and more chaotic than the previous cases. This can be recognized from the varying amplitude of displacements with maximum trough at approximately 400 mm.

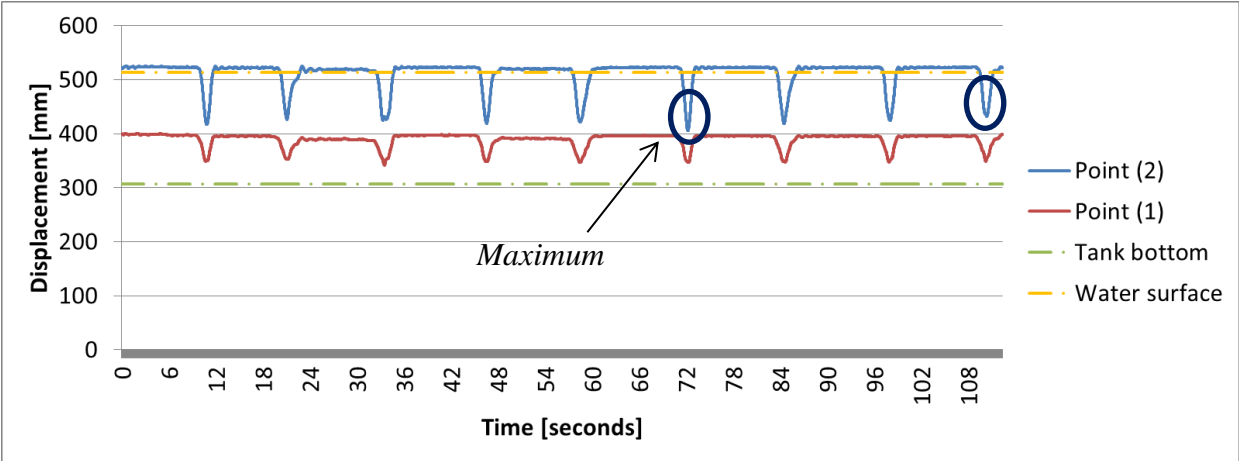


Figure (5. 16): More chaotic motion pattern of case (3)

The simulations results of case (3) are shown in figure (5.17). The figure shows a similar chaotic behavior as in the experiment. The amplitude of oscillations has also reduced compared to simulations from cases (1) and (2).

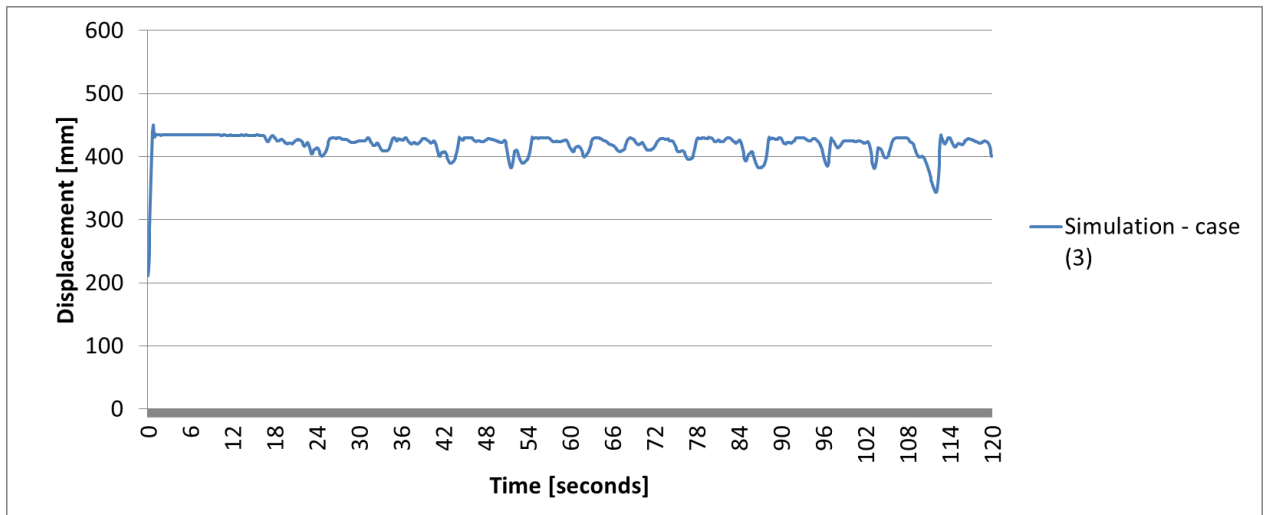


Figure (5. 17): Simulation results for case (3) showing similar chaotic behavior and less displacement amplitudes [19]

2.4 – Case (4)

The displacements behaved more uniformly again similar to cases (1) and (2) as shown in figure (5.18). The amplitude of displacements increased again reaching the tank bottom. The liquid filling is faster than case (1) and the displacements frequency almost same as in case (3).

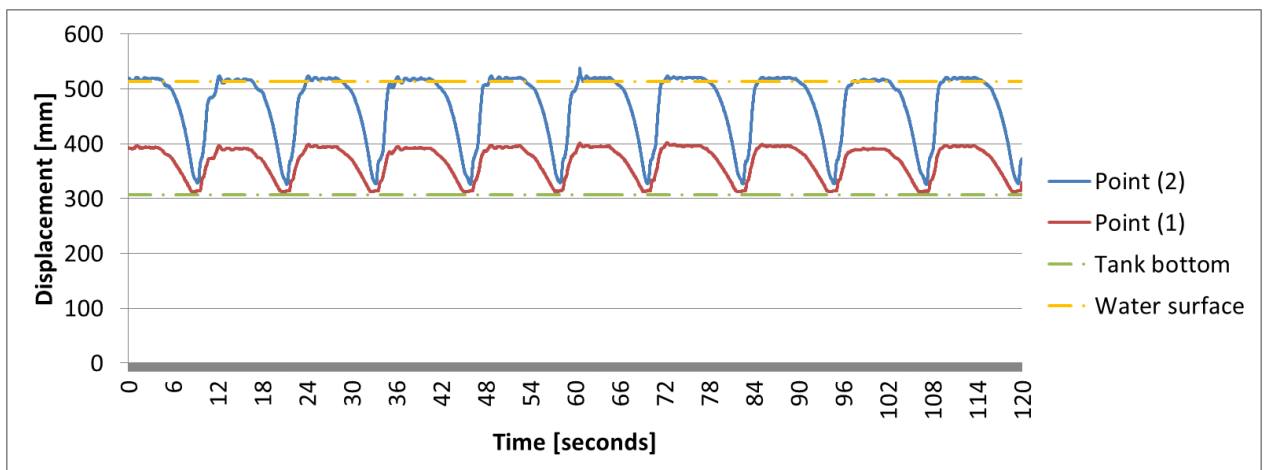


Figure (5. 18): Motion pattern of case (4) with more uniform behavior as in cases (1) and (2)

Figure (5.19) shows the simulation results for case (4). The figure shows that the amplitude of displacements has increased compared to simulation of case (3). However the figure shows that the motion behavior is chaotic compared to experimental results. The figure shows also high oscillating frequency.

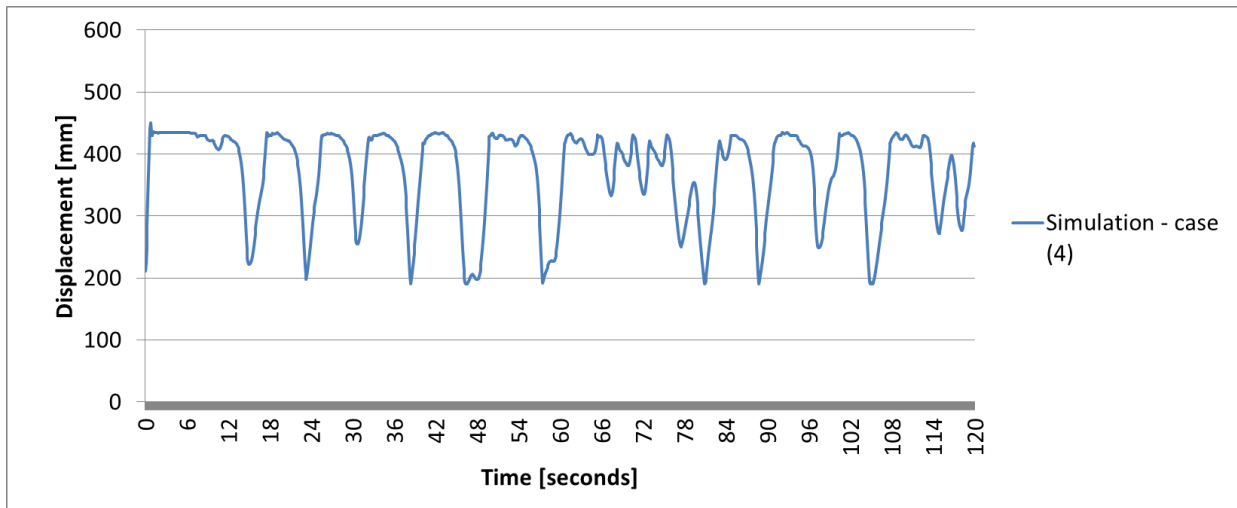


Figure (5. 19): Simulation results for case (4) [19]

3 Discussion

The results showed that the structural behavior of the hose for this geometry is strongly depending on balance between gas and liquid superficial velocities. When gas velocity is much higher, the experiments showed more chaotic behavior and less displacement. However when the liquid superficial velocity was increased over the gas velocity, the system showed a uniform behavior and hose remained on tank bottom for longer time.

Although simulation results of the four cases did not show exactly a perfect matching motion behavior, the pattern was almost same. The dynamic response of the riser in simulations was similar to the experiments relative to change in superficial velocities.

An interesting transition between stratified and elongated bubble flow regime was observed prior to the liquid filling stage. After liquid accumulates and passes over detected point (2), gas blows again in the form of stratified flow.

Conclusion

Small scale experiments were carried out in the lab for studying the effect of two-phase flow on dynamic behavior of flexible pipes. Air and water were supplied through a mini-loop instrumentation box. Geometries investigated were cantilever hose in vertical and horizontal position and DWH riser accident case. The experiments showed an interaction between structural behavior of flexible pipes and flow superficial velocities. The experimental results were compared to simulations from structural dynamics analysis code.

Experiments were carried out at air and water flow rates limited to the compressor and pump capacities. Although the experiments showed good dynamic response in case of horizontal cantilever hose, the response in vertical geometry was limited to vibrations. Testing the vertical cantilever hose at higher flow rates may reveal more dynamic behavior than one presented here. It was observed that liquid slugs have an effect on oscillating behavior of cantilever hoses. The liquid slugs momentum is dominated by gas superficial velocity. Change in liquid superficial velocity had an effect on oscillation frequency of the hoses.

Experiments with DWH riser showed different flow regimes including slugging, stratified and elongated bubble. The same oscillating motion of the riser was reproduced in the lab. However, the two-phase flow pattern observed in the laboratory is different from that introduced in the accident investigation report [4]. There are many parameters that have an influence on experiment such as liquid surface tension, gas density and geometry scale. At high gas velocity, the motion was more chaotic and hose was oscillating with small displacement amplitudes.

It was observed that silicon hoses are good option for detailed investigation of structural behavior. With low bending stiffness, they are flexible enough to demonstrate the effect of internal flow forces that result in the oscillation of the hose.

Recommended Future Work

- The cantilever experiments can be carried out underwater for studying the effect of water drag on oscillations.
- An experimental loop can be arranged to test slug flow in a rigid system of pipes with elbows at different angles. This may provide an opportunity for studying flow pressures across the elbows which can reveal more information about structural interaction with internal fluid flow.
- With higher flow rates, it is possible to test the cantilever geometry with hoses of higher bending stiffness and rigid pipes. This may demonstrate the effect of structural damping of the pipes on fluid-elastic instability.
- Investigating the experimental results with simulations from a commercial software package would give an opportunity for verifying more simulations.
- After the completion of new tank construction, floating pipe geometry with external force can be tested. The external force here represent a ship connected to a riser, the case is a two-way coupling between internal flow and external force.
- Investigating pigging in flexible pipes is a strong potential for future research.

References

- [1] PSA, Norway (2013). " Un-bonded Flexible Risers – Recent Field Experience and Actions for Increased Robustness". Document no. 0389-26583-U-0032. Project no. 0389
- [2] Eni Norge (2013). Annual Report. Stavanger: Eni Norge AS. URL; http://www.eninorge.com/Documents/Rapporter/ENI_%C3%A5rsrapport%202013.PDF
- [3] SPE News | Macondo Modeling Indicates Lower Discharge. 2015. *SPE News / Macondo Modeling Indicates Lower Discharge*. [ONLINE] Available at: <http://www.spe.org/news/article/modeling-of-macondo-slug-flow-indicates-lower-total-discharge-of-oil>. [Accessed 12 May 2015].
- [4] Michael Zaldivar (2013), "Quantification of Flow Rate during Slug Flow". URL; <http://www.mdl2179trialdocs.com/releases/release201310161045010/TREX-011683.pdf>
- [5] Hanratty, T. J. , 2013. *Physics of Gas-Liquid Flows*. 1st ed. New York, US: Cambridge University Press.
- [6] Baliño, J. L. (2014). "Modeling and simulation of severe slugging in air-water systems including inertial effects." *Journal of Computational Science* 5(3): 482-495.
- [7] Ortega, A., Rivera, A., & Larsen, C. M. (2013). " Flexible riser response induced by combined slug flow and wave loads. " International conference on Ocean, Offshore and Arctic Engineering, 10.
- [8] Ortega, A., et al. (2012). "On the Dynamic Response of Flexible Risers Caused by Internal Slug Flow." Proceedings of the Asme 31st International Conference on Ocean, Offshore and Arctic Engineering, 2012, Vol 5: 647-656.
- [9] Dahman, J. S., Fujimoto, R. M. & Weatherly, R. M. The department of defense high level architecture. *1997 Winter simulation conference*
- [10] VIEIRO, J. J., Amr M. Hemedad and Ole Jørgen Nydal (2015). MULTIPHASE FLOW IN FLEXIBLE PIPES: COUPLED DYNAMIC SIMULATIONS AND SMALL SCALE EXPERIMENTS ON GARDEN HOSE INSTABILITY. *In The 8th National Conference on Computational Mechanics - MekIT'15*. Trondheim, Norway, 2015. Trondheim: NTNU. 10.

- [11] Harvard University. 2015. [ONLINE] Available at: http://ipl.physics.harvard.edu/wp-uploads/2013/03/PS3_Error_Propagation_sp13.pdf. [Accessed 12 June 2015].
- [12] Monette, C. and M. J. Pettigrew (2004). "Fluidelastic instability of flexible tubes subjected to two-phase internal flow." Journal of Fluids and Structures **19**(7): 943-956.
- [13] Chen, S. S. and J. A. Jendrzejczyk (1981). "Experiments on Fluid Elastic Instability in Tube Banks Subjected to Liquid Cross Flow." Journal of Sound and Vibration **78**(3): 355-381.
- [14] Gregory, R. W. and Paidouss.Mp (1966). "Unstable Oscillation of Tubular Cantilevers Conveying Fluid .2. Experiments." Proceedings of the Royal Society of London Series a-Mathematical and Physical Sciences **293**(1435): 528-&.
- [15] Paidouss, M. P. (1970). "Dynamics of Tubular Cantilevers Conveying Fluid." Journal of Mechanical Engineering Science **12**(2): 85-&.
- [16] Benjamin, T. B. (1961). "Dynamics of a System of Articulated Pipes Conveying Fluid .1. Theory." Proceedings of the Royal Society of London Series a-Mathematical and Physical Sciences **261**(1304): 457-+.
- [17] Yoon, J., et al. (2006). "Flow-induced flutter instability of cantilever carbon nanotubes." International Journal of Solids and Structures **43**(11-12): 3337-3349.
- [18] Math Works (2012), Computer Vision System Toolbox, User's Guide.
- [19] Simulations data from Joaquin Vieiro as part of PhD work to be published in the future.
- [20] Ibrahim, R. A. (2011). "Mechanics of Pipes Conveying Fluids-Part II: Applications and Fluidelastic Problems." Journal of Pressure Vessel Technology-Transactions of the Asme **133**(2).

Appendix (A): Presented Paper for Publishing

MULTIPHASE FLOW IN FLEXIBLE PIPES: COUPLED DYNAMIC SIMULATIONS AND SMALL SCALE EXPERIMENTS ON GARDEN HOSE INSTABILITY

Joaquin J. Vieiro, Amr M. Hemedat AND Ole J. Nydal

Department of Energy and Process Engineering
Norwegian University of Science and Technology (NTNU)
Kolbjørn Hejes v 1B, NO-7491 Trondheim, Norway
e-mail: joaquin.vieiro.medina@ntnu.no, www.ntnu.edu/ept

Key words: Fluid-structure interaction, two-phase flow, flexible pipes, garden hose instability

Abstract. The garden hose instability is a characteristic phenomenon of fluidelastic instability on flexible pipes conveying fluids. It consists in pipe fluttering due to internal flow induced forces on the pipe wall. In order to study this phenomenon, some small scale experiments of water and air-water two-phase flow through a open ended flexible pipe were carried out. The experiments are compared with numerical simulations using a coupled flow and structure model. The model solves both multiphase flow and structure dynamics in the time domain. The dynamics of an open ended pipe is reproduced in the simulations.

1 INTRODUCTION

Flexible pipes are often used in offshore oil and gas production systems to transport the well fluids from the seabed to surface facilities. These flexible pipes are exposed to multiple external loads like sea current drag, vortex shedding induced forces, waves and seabed interaction as well as internal fluid loads. Under certain conditions, the produced gas and liquid may exhibit intermittent liquid and gas flow (slug flow), potentially causing large variation in pipe tension and large motion due to the internal flow dynamics [1].

Two-way fluid-structure interaction simulations on flexible risers have been demonstrated by Ortega *et al.* [2, 3], reporting important effects of slug flow on the structural dynamic but without comparisons with experimental or full scale field data.

Due to the lack of full scale measurements of the impact of internal multiphase flow in pipeline-riser systems, a small scale experiment has been designed in the NTNU Multiphase Flow Laboratory. The experiment involves fluidelastic instabilities as the one observed in a garden or fire hose which is left free over a smooth surface.

2 NUMERICAL MODEL

In this section the main features of the internal fluid flow simulator as well as the basic equations of the structural dynamic model are presented. Finally, the coupling procedure of the two models is described.

2.1 Fluid dynamics

The internal flow was solved using a one-dimensional two-fluid model based on a slug tracking model formulation [4]. A dynamic mesh describes the bubbles and slugs regions and each of these regions can have a subgrid (sections) as shown in Figure 1.

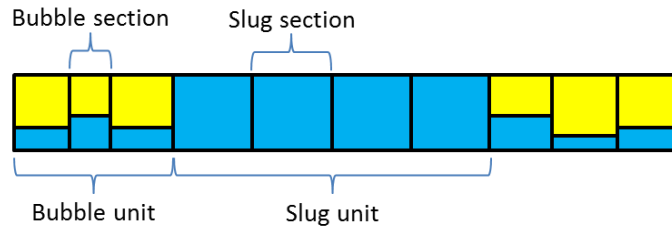


Figure 1: Mesh elements in the slug tracking scheme

The slug units are solved as incompressible fluid and the gas units as compressible using the two fluid model [4], i.e. mass, momentum and energy equations are solved for each phase. The mass equations give the phase fractions. A state equation is required for the gas region. The liquid slug formation can be captured directly from the two-fluid model on a stationary grid, and the slugs and bubbles are tracked thereafter with a moving grid.

The general mass conservation equation for a fluid phase k is expressed by:

$$\frac{\partial \alpha_k \rho_k}{\partial t} + \frac{\partial (\alpha_k \rho_k U_k)}{\partial \Lambda} = \Psi_k \quad (1)$$

where α is the volume fraction, ρ is the density, U is the average velocity, Ψ is the mass transfer terms, t is the time variable and Λ is the pipe longitudinal axis coordinate. The momentum equation for a phase k is given by:

$$\frac{\partial (\alpha_k \rho_k U_k)}{\partial t} + \frac{\partial \alpha_k \rho_k U_k^2}{\partial \Lambda} = -\alpha_k \frac{\partial p}{\partial \Lambda} - F_{wall,k} \pm F_{int,k} - G_k \quad (2)$$

where \mathbf{p} is the pressure field, $\mathbf{F}_{wall,k}$ is the friction force between phase \mathbf{k} and the pipe wall, $\mathbf{F}_{int,k}$ is the friction force between phase \mathbf{k} and its interphase with another phase, and \mathbf{G} is the gravity force, including a term to take into account a level gradient force. Details about extension of these conservation equations to the slug tracking framework can be found in [5].

2.2 Structural dynamics

The model presented here is based on the lumped mass method shown by [6] and extended to consider structural damping and internal flow forces. The pipeline is divided into an arbitrary number of elements, connected in sequence by their nodes. The mass of each element and the fluids contained in it are lumped equally on the two nodes at which it is connected to. The node position \vec{s}_i , velocity \vec{v}_i , and acceleration \vec{a}_i relative to a stationary coordinate system are defined with three dimensional vectors as follows:

$$\vec{s}_i = \begin{Bmatrix} x_i \\ y_i \\ z_i \end{Bmatrix} \quad \vec{v}_i = \dot{\vec{s}}_i \quad \vec{a}_i = \dot{\vec{v}}_i \quad (3)$$

where subscript i represents the node number. The pipe structural properties (stiffness and damping) were modeled as massless springs and dampers as shown on Figure 2.

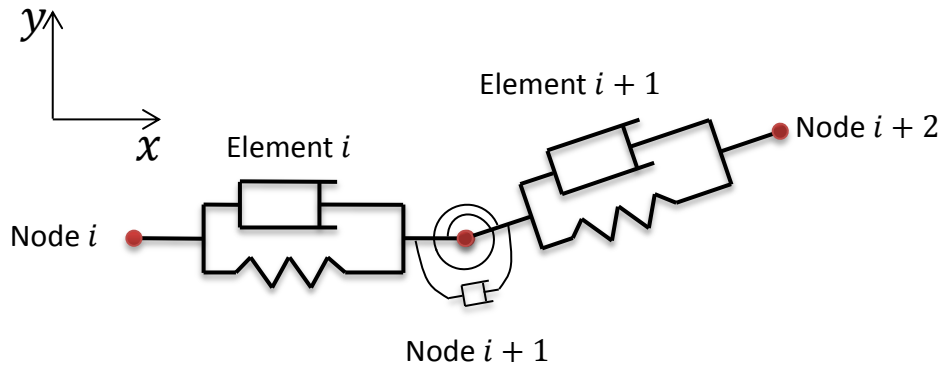


Figure 2: Schematic representation of the mechanical system

The dynamic equilibrium equation for each node is as follows:

$$m_i \vec{a}_i = \vec{F}_i \quad (4)$$

The term m_i represents the lumped mass on node i . The right hand term Eq. 4 includes representative forces, in this case: internal structure forces (stiffness and damping), gravity, soil friction, internal fluid friction and centrifugal forces. The contribution of internal flow to damping [7] was not included. There is no backward reaction force due to ejected fluid as explained by [8]. Time integration of Equation 4 was performed by Newmark beta method [9].

2.3 Fluid-structure coupling

The fluid-structure coupling was done as follows:

- The fluid equations are solved and the fluid mesh is updated. All fluid parameters are updated on each fluid cell.
- Considering that a structural cell may cover a variable number of fluid cells, some calculation must be done in order to get appropriated values of fluid fields on each structural element such as velocity, volume fraction and contained mass.
- The fluid-wall friction force was obtained from the fluid dynamics solver and the centrifugal force was calculated as the variation of the momentum across nodes for each fluid phase.
- The total force is updated and the structural equations are solved. The system geometry is updated according to the calculated displacements.
- Move one time step forward and repeat the calculation steps above until final time is reached.

3 TEST CASE

In order to validate the coupled fluid-structure interaction model, a small-scale experiment was selected. The test consisted on a flexible hose laid on a smooth horizontal surface conveying air-water flow. Details about the experimental setup and simulation configuration are given in the following sections.

3.1 Experimental setup

The experiments have been carried out using a silicon hose of 6 mm internal diameter and 9 mm external diameter. Air and water were supplied using an air compressor and centrifugal pump. The two fluids are mixed in a symmetric “Y” fitting. One end of the hose was clamped and the other one was free to move. The hose was laid over a smooth acrylic sheet covered with a soap-water mixture in order to reduce friction. Figure 3 shows a schematic diagram of the experimental apparatus used for the experiment.

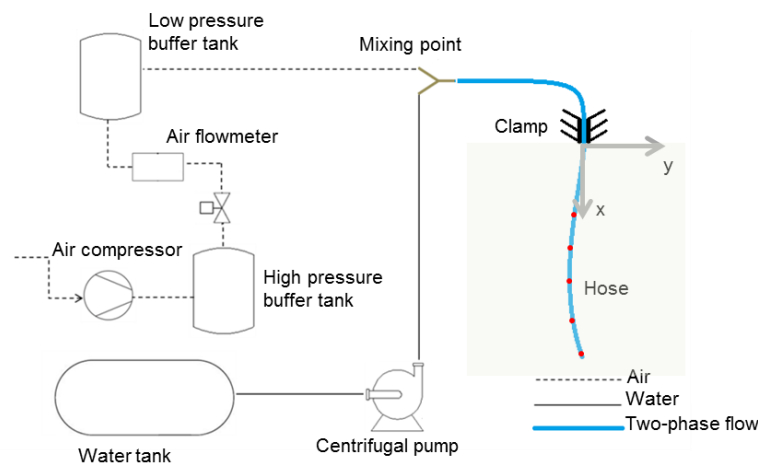


Figure 3: Experimental assembly

The air and water mass flow rates were set to 0.24 g/s and 16.52 g/s respectively (liquid and gas superficial velocities of 0.58 m/s and 6.78 m/s). Fluttering was obtained under there conditions. The movement of the hose was recorded by using a digital camera. Three frames are shown in Figure 4. A tracking algorithm was applied to the video in order to obtain the position of five prestablised points on the hose (Figure 5). The displacement of those five points over the horizontal plane with origin on the clamped point are plotted on Figure 6.

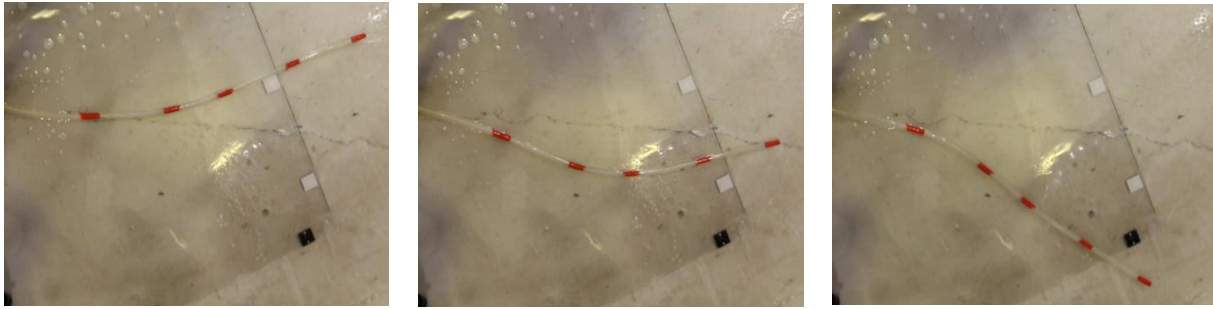


Figure 4: Selected frames extracted from experiment video

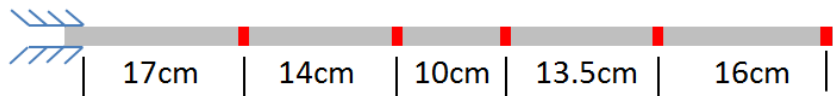


Figure 5: Distribution of tracked points along the hose

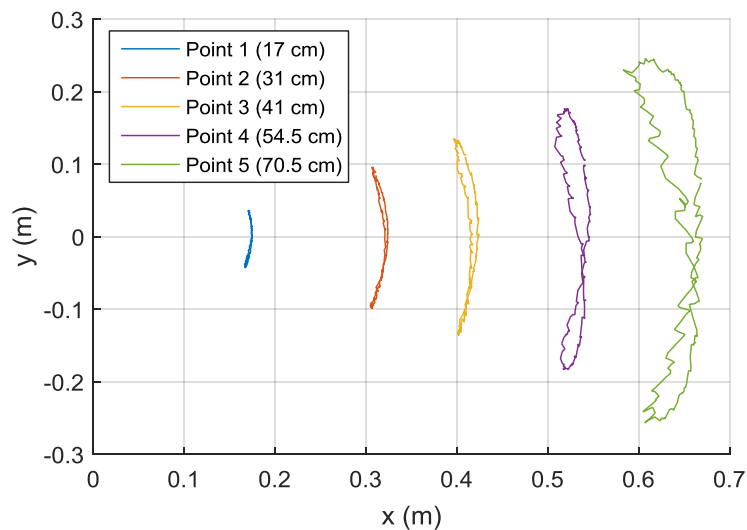


Figure 6: Trajectories of tracked points during the experiment

From video analysis it was also possible to obtain a slug frequency of approximately 3.3 slugs per second.

3.2 Simulation setup

The hose was modeled as 36 structural sections of 2cm each. The bending stiffness and damping coefficient were estimated by the method described in the appendix. The main parameter set to the fluid and structural solvers are presented in Table 1, Table 2 and Table 3.

Table 1: Fluid simulation main parameters

Water mass flow rate (g/s)	16.52
Air mass flow rate (g/s)	0.24
Outlet pressure (kPa)	101
Holdup for slug initiation (-)	0.43
Air buffer tank volume (cm ³)	600
hose Internal diameter (mm)	6
Roughness (mm)	0.01

Table 2: Fluid solver spatial and temporal meshes

Minimum slug (mm)	6
Minimum bubble (mm)	10
Maximum bubble (mm)	50

Table 3: Structural simulator main parameters

Mass per unit length (g/m)	44
Bending stiffness (N m ²)	0.003
Axial stiffness (Pa)	500
Maximum time step (s)	1e-4
Element length (mm)	20
Kinetic friction coefficient (-)	0.3

Due to the limitations of the fluid dynamic model to reproduce surface tension effects on small diameter pipes, the slug initiation holdup (liquid volume fraction) was set to 0.43 in order to stimulate the slug generation. This configuration produced around 3 slugs per second. The liquid holdup time series at the outlet between 23 and 25 seconds is plotted on Figure 7.

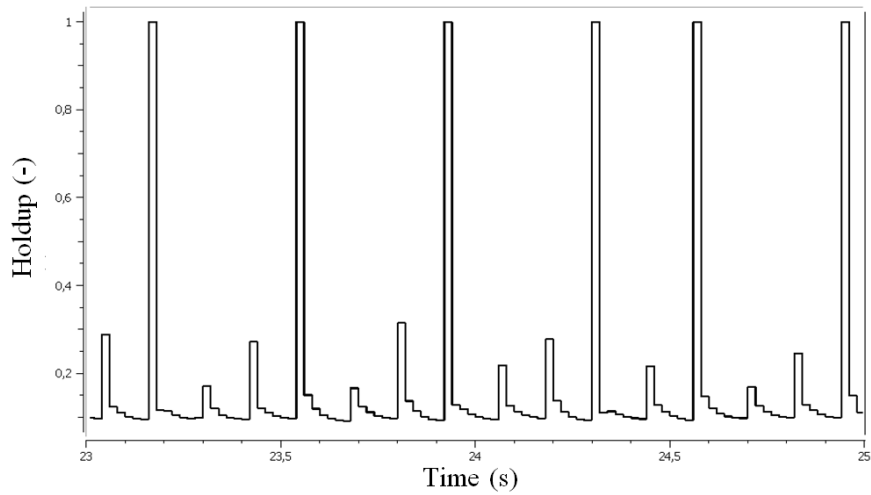


Figure 7: Simulated holdup time series at outlet

4 RESULTS AND DISCUSSIONS

The simulation results reproduced the fluttering behavior observed on the experiment. Six representative pipe shapes during a same flutter cycle are shown in Figure 8. The trajectories of five points nearby the ones tracked in the experiment are presented on Figure 9. The maximum deflection from the straight configuration was over-predicted in 50%.

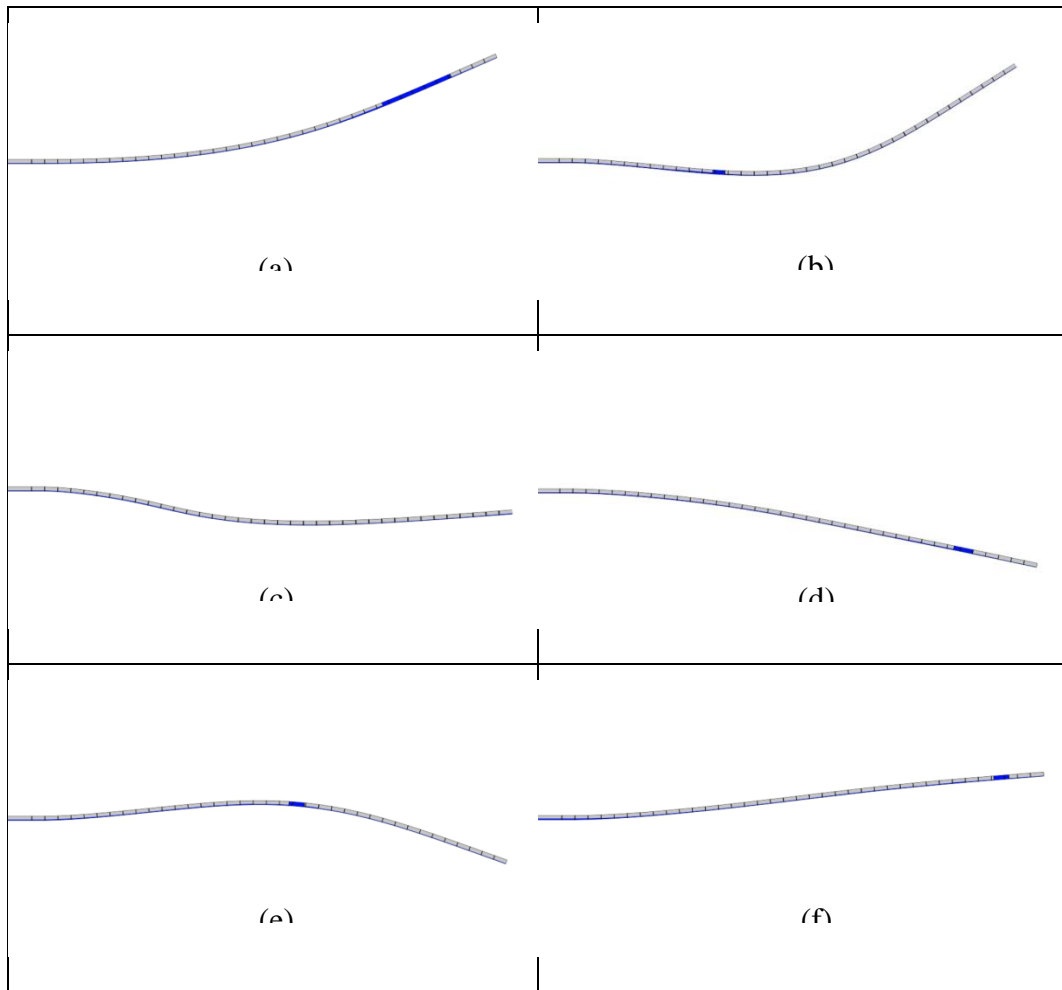


Figure 8: Selected frames extracted from simulation results

The period of fluttering was also compared and in this case, it was under-predicted by 30%. Figure 10 shows experimental and simulated time series corresponding to the farthest tracked point from the clamped point.

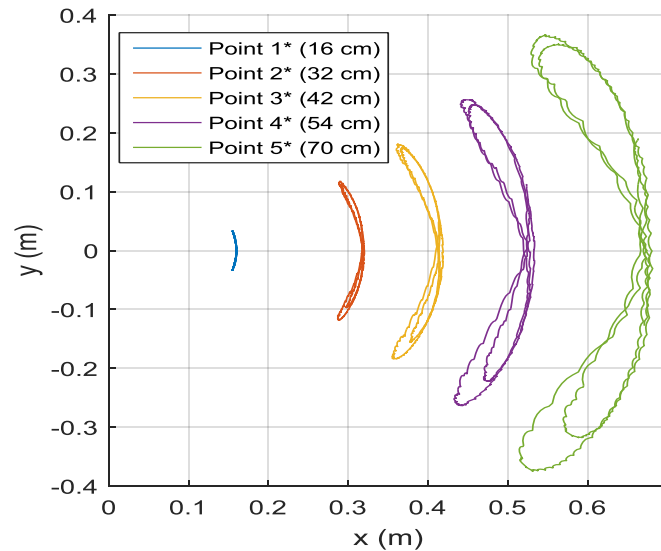


Figure 9: Trajectories of tracked points from the simulation

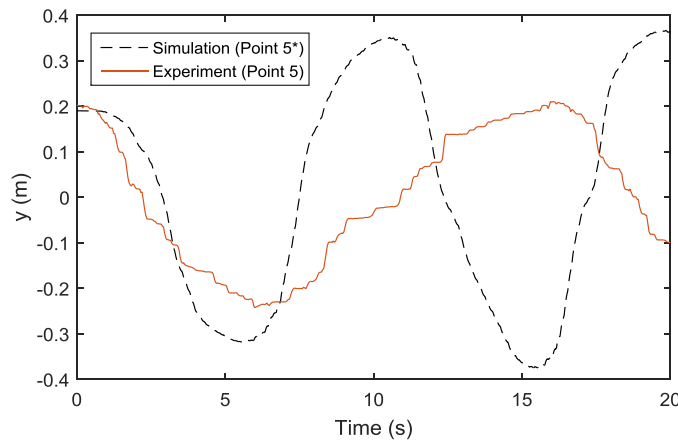


Figure 10: Traversal displacement of points 5 and 5* over 20 s

The wider “8” shape described by the trajectory of almost all the tracked points indicate a larger hose curvature on the simulated results. This may indicate a wrong estimation of bending damping by neglecting the internal flow induced damping.

Although a quantitative analysis of the predicted displacement can be improved, the presented model demonstrates important details of the dynamics of the fluid-structure interaction.

It is worth to note that some of the parameters introduced in the simulation like friction coefficient and slug initiation holdup were estimated due to lack of information on the experiment conditions or model limitations.

6 CONCLUSIONS

- Experiment and simulations of a fluid-structure interaction case were carried out on a horizontal cantilever pipe conveying air-water slug flow.

- The implemented fluid-structure interaction model reproduced qualitatively the physics of a flexible pipe conveying gas-liquid flow.
- Differences in amplitude and oscillation period may be a consequence of not including two-phase internal fluid induced damping. The results will also be dependent on slug initiation models for small diameter pipes, as well as the friction between pipe and surface.

ACKNOWLEDGMENT

Project / research funded by VISTA – a basic research program and collaborative partnership between The Norwegian Academy of Science and Letters and Statoil.

REFERENCES

- [1] F. B. Seyed and M. H. Patel, "Considerations in Design of Flexible Riser Systems," presented at the Proceedings of the Second (1992) International Offshore and Polar Engineering Conference, San Francisco, USA, 1992.
- [2] A. Ortega, A. Rivera, O. J. Nydal, and C. M. Larsen, "On the Dynamic Response of Flexible Risers Caused by Internal Slug Flow," presented at the ASME 2012 31st International Conference on Ocean, Offshore and Arctic Engineering, Rio de Janeiro, Brazil, 2012.
- [3] A. Ortega, A. Rivera, and C. M. Larsen, "Flexible Riser Response Induced by Combined Slug Flow and Wave Loads," presented at the ASME 2013 32nd International Conference on Ocean, Offshore and Arctic Engineering, Nantes, France, 2013.
- [4] O. J. Nydal, "Dynamic Models in Multiphase Flow," *Energy & Fuels*, vol. 26, pp. 4117-4123, 2012.
- [5] T. K. Kjeldby, "Lagrangian three-phase slug tracking methods," Ph.D. Doctoral thesis, Department of Energy and Process Engineering, Norwegian University of Science and Technology (NTNU), Trondheim, 2013.
- [6] R. Ghadimi, "A Simple and Efficient Algorithm for the Static and Dynamic Analysis of Flexible Marine Risers," *Computers & Structures*, vol. 29, pp. 541-555, 1988.
- [7] A. Gravelle, A. Ross, M. J. Pettigrew, and N. W. Mureithi, "Damping of tubes due to internal two-phase flow," *Journal of Fluids and Structures*, vol. 23, pp. 447-462, 4// 2007.
- [8] F. Vera, Rivera, R., Nuñez, C., "Backward Reaction Force on a Fire Hose, Myth or Reality?," *Fire Technology*, pp. 1-5, 2014/08/28 2014.
- [9] R. Clough, Penzien, J., *Dynamics of Structures*, Third ed.: Computers & Structures, Inc., 2003.

APPENDIX

The hose bending stiffness and damping coefficient were estimated as follows: the hose was installed as a vertically hanging cantilever. The free end was displaced and released to trigger pendulum oscillations. The previously mentioned video recording and processing technic was employed to track the free end of the hose during the experiment. Then the period of oscillation and logarithmic decrement of amplitude were calculated. The same experiment was simulated in the structural dynamic software described on section 3.1. Different values of bending stiffness and damping coefficient were tested until obtaining results fairly close to the experiment. Figure 11 presents the amplitude per cycle measured from the experiment and the simulation results with a bending stiffness of 0.001 N m^2 .

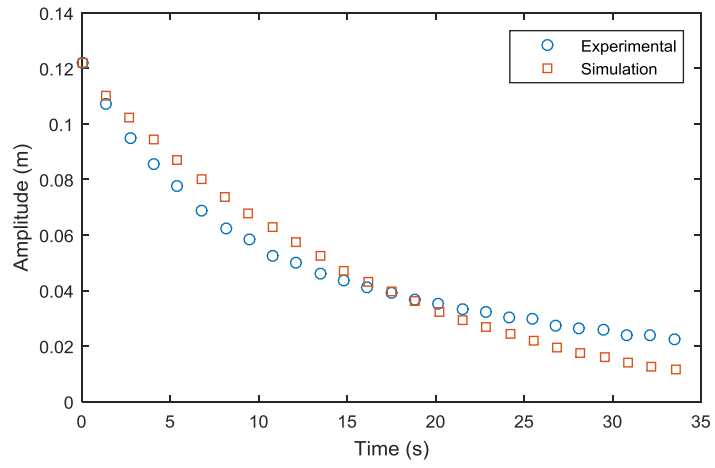


Figure 11: Calibration of bending stiffness. Measured and simulated amplitude of oscillation of a hanging pipe

Appendix (B): MATLAB Code

```
clear;
clc;
% Construct an object to read video data from a file
vidIn = VideoReader('MVI_7108.mov');

% This creates a looping through the frames of the experiment
video

for ii = (1:vidIn.NumberOfFrames);
%for ii = (1:500);
    %x = vidIn.FrameRate;
    % Reading the frames of the video indexed by
    NumberOfFrames
    pic = read(vidIn, ii);
    imshow(pic)
    % For every frame captured, the red object is subtracted
    from the background image
    % to recognize the red object target
    diff_im = imsubtract(pic(:,:,1), rgb2gray(pic));
    % Median filtering for matrix diff_im in 2D, each output
    pixel contains
    % the median value in the 3x3 neighborhood around
    corresponding pixel in input image
    diff_im = medfilt2(diff_im, [3 3]);
    % Convert from grayscale into binary, the o\p image bw
    replaces all
    % pixels in i\p image with luminance greater than 0.18
    with value 1 (black) and
    % replaces all other pixels with value 0 (white)
    diff_im = im2bw(diff_im,0.18);
    % Remove all objects that have fewer than 300 pixels
    diff_im = bwareaopen(diff_im,300);
    % Returns a matrix bw containing labels for 8-connected
    objects
    bw = bwlabel(diff_im, 8);
    stats = regionprops(bw, 'BoundingBox', 'Centroid');
    %imshow(pic)
    hold on
```

```

    %This is a loop to bound the red objects in a rectangular
    box.

    % length returns the length for the largest array
    dimension in stats
    %%
    for object = 1:length(stats)
        % BoundingBox is smallest rectangle containing the
        region
        bb = stats(object).BoundingBox;
        % Centroid specifies the center of mass of the region
        bc = stats(object).Centroid;
        % rectangle draws a rectangle with Position [0,0,1,1]
        and Curvature [0,0] (i.e., no curvature)
        rectangle('Position',bb,'EdgeColor','r','LineWidth',2)
        plot(bc(1),bc(2), '-m+')
        a=text(bc(1)+15,bc(2),          strcat('X:          '),
num2str(round(bc(1))), '      Y: ', num2str(round(bc(2))));
        set(a, 'FontName', 'Arial', 'FontWeight', 'bold',
'FontSize', 12, 'Color', 'yellow');

        temp(ii,:,object)= bc;
        temp1 = round(temp);

    end
    hold off
end
f = getframe
imshow(pic);
sprintf('%s','Simulation Done ')

```